

26071004

Cosponsored
U. S. Army Material Command
Projects Nos. 1-V-O-14501-B-52A-30
and 1-V-O-21701-A-046-05
and
Directorate of Remote Area Conflict
Advanced Research Projects Agency
ARPA Order No. 400
Contract No. DA-22-079-eng-330
with
U. S. Army Engineer Waterways Experimental Station

Research in Earth Physics

Phase Report No.2

**ADSORPTION AND FRICTION
BEHAVIOR OF MINERALS
IN VACUUM**

COPY	OF	96 1'
HARD COPY	\$.	300
MICROFICHE	\$.	600

Leslie G. Bromwell

DDC
JUN 25 1965

Research Report R64-42

EVALUATION COPY
March, 1965
PROCESSING

MIT

**DEPARTMENT
OF
CIVIL
ENGINEERING**

SCHOOL OF ENGINEERING
MASSACHUSETTS INSTITUTE OF TECHNOLOGY
Cambridge 39, Massachusetts

**ADSORPTION AND FRICTION BEHAVIOR
OF MINERALS IN VACUUM**

**Research in Earth Physics
Phase Report No. 2**

by

Leslie G. Bromwell

March 1965

Cosponsored

by

**U.S. Army Materiel Command
Projects Nos. 1-V-0-14501-B-52A-30
and 1-V-0-21701-A-046-05**

and

**Directorate of Remote Area Conflict
Advanced Research Projects Agency
ARPA Order No. 400**

under

Contract No. DA-22-079-eng-330

with

**U.S. Army Engineer Waterways Experiment Station
CORPS OF ENGINEERS
Vicksburg, Mississippi**

**Soil Mechanics Division
Department of Civil Engineering
Massachusetts Institute of Technology**

Research Report R64-42

ABSTRACT

This report presents theoretical considerations on the adsorption and friction behavior of soils under high vacuum and extreme temperature conditions. It includes an extensive literature survey, particularly in the fields of surface chemistry and physics, adsorption, and friction.

The importance of using clean, reproducible surfaces for surface studies is demonstrated. The necessity of clean ultra-high vacuum test conditions for producing and maintaining clean surfaces is emphasized. The relationship between atomic forces and surface energy and the friction and adhesion between solid surfaces is discussed. A theoretical relationship between adsorption energy and the temperature and pressure required to remove adsorbed layers is derived.

The frictional behavior of quartz is considered in detail. It is concluded that significant increases in the coefficient of friction, and thereby the shear strength, of particulate mineral systems will result if adsorbed contaminants are removed. However, in the absence of a mechanism for producing a large contact area, significant cohesion will not develop.

FOREWORD

The work described in this report was performed under Contract No. DA-22-079-eng-330 entitled "Research Studies in the Field of Earth Physics" between the U.S. Army Engineer Waterways Experiment Station and the Massachusetts Institute of Technology. The research is cosponsored by the U.S. Army Materiel Command under DA Projects 1-V-0-14501-B-52A-30, "Earth Physics (Terrain Analysis)," and 1-V-0-21701-A-046-05, "Mobility Engineering Support," and by the Directorate of Remote Area Conflict, Advanced Research Projects Agency, under the "Mobility Environmental Research Study," ARPA Order No. 400.

The general objective of the Research in Earth Physics is the development of a fundamental understanding of the behavior of particulate systems, especially cohesive soils, under varying conditions of stress and environment. Work on the project, initiated in May, 1962, has been carried out in the Soil Mechanics Division (headed by Dr. T. William Lambe, Professor of Civil Engineering) of the Department of Civil Engineering under the supervision of Dr. Charles C. Ladd, Associate Professor of Civil Engineering.

This report presents only one portion of the overall research being conducted under the contract. Other phases currently under investigation are:

1. In Situ Strength and Compression Properties of Natural Clays.
 - (a) Effects of sample disturbance (i.e. excessive shear strains) on the undrained strength, stress-strain modulus, and one-dimensional compression behavior of natural clays.

- (b) Effects of stress-system variables (anisotropic consolidation, intermediate principal stress, rotation of principal planes) on stress-strain behavior of clays during undrained shear.

2. Influence of Environment on Strength and Compression Properties of Soils.

- (a) Effect of high vacuum and temperature on the properties of granular systems.
- (b) Effects of natural cementation and type of pore fluid on the strength and compression properties of saturated clays.
- (c) The strength of clays at very low effective stresses and especially the nature and magnitude of "true cohesion".

3. The Structure of Clay.

- (a) Nature and magnitude of interparticle forces in clay-water systems.
- (b) Fabric of kaolinite.

Many of the above topics complement and/or draw information from other research projects in the Soil Mechanics Division. These include support from the Office of Naval Research and the National Science Foundation (Grant G-19440).

This report was prepared by Mr. Leslie G. Bromwell, N.A.S.A. Fellow, under the supervision of Professor Ladd. Dr. R. Torrence Martin, Research Associate in the Soil Mechanics Division, reviewed the report and offered technical assistance on many phases of the work. The information contained in the report has served as the basis for the formulation of the experimental portion of this study which is currently underway, the results of which will be presented in a later report.

**Pertinent reports issued under this research contract
are:**

- 1. "Research in Earth Physics, Progress Report for the
Period June 1962 - December 1962", Department of
Civil Engineering Publication R63-9, M.I.T. Feb. 1963.**
- 2. Ladd, C. C., "Stress-Strain Behavior of Saturated Clay
and Basic Strength Principles", Phase Report No. 1,
Part 1, Department of Civil Engineering Publication
R64-17, M.I.T. April, 1964.**

TABLE OF CONTENTS

	page
I. INTRODUCTION	9
A. Purpose of Report	9
B. Background	9
II. THE USE OF HIGH VACUUM TO STUDY SURFACE PHENOMENA	13
A. Introduction	13
B. Preparing Clean Surfaces	14
C. The Degree of Cleanliness of a Vacuum	19
D. Conclusions	22
III. THE SOLID SURFACE	25
A. Nature of the Solid Surface	25
B. Surface Forces and Surface Energy	28
IV. ADSORPTION ON SOLID SURFACES	37
A. Atomic Forces and Adsorption	37
B. Surface Energy and Adsorption Energy	38
C. The Nature of the Adsorbed Layer	40
D. Desorption of Surfaces Under High Vacuum	46
V. FRICTION AND COHESION OF SOLID SURFACES	56
A. The Adhesion Theory of Friction	57
B. Theory of Friction for Elastic Solids	60
C. Friction and Cohesion of Clean Surfaces	67
D. The Frictional Behavior of Minerals	70
VI. PREVIOUS HIGH VACUUM RESEARCH ON SOILS	78
VII. CONCLUSIONS	83

	page
VIII. LITERATURE CITED	85
Appendix I. PURGING ACTIVE GASES FROM HIGH VACUUM SYSTEMS	91
Appendix II. KINETICS OF SURFACE DESORPTION	94

<u>LIST OF TABLES</u>	page
III-1 Measured and Theoretical Values of Surface Energy	34
IV-1 Adsorption Times for Various Adsorption Energies	51
<u>LIST OF FIGURES</u>	
II-1 Time to Form a Monolayer of Coverage vs Gas Pressure	23
-2 Ultimate Pressure vs Pumping Speed	24
-3 Contamination of Glass by Diffusion Pump Oil	24
III-1 Contact between Two Smooth Surfaces	35
-2 Surface Structure of a Polished Crystalline Solid	35
-3 The Surface Energy of Solids	36
IV-1 The Surface of Quartz	52
-2 Pressure Required to Remove an Adsorbed Layer	53
-3 Temperature and Pressure Conditions for Desorption	54
-4 Desorption of a Quartz Surface	55
-5 Evolution of Water from Glass	55
V-1 Friction as a Function of Interfacial Strength	74
-2 Area Increase vs F/W	74
-3 Variation of Friction with Particle Size	75
-4 Friction as a Function of Load per Particle	75
-5 Mohr Envelope for Quartz	76
-6 Coefficient of Friction vs Load for Mica	77
-7 Area of Contact vs Friction Force for Mica	77

I. INTRODUCTION

A. Purpose of Report

This is the first phase report on the behavior of soils under high vacuum and extreme temperature conditions. It includes the results of an extensive literature survey of the fields relating to soils under high vacuum, particularly those of surface chemistry and physics, adsorption, and friction. It also presents conclusions drawn by the author, based on this survey and on theoretical calculations. This material has served as the basis for the design of equipment for the experimental part of the project, the results of which will be presented in a later report.

The conclusions reached in this report will serve as a guide for planning future experimental work in this area.

B. Background

The primary purpose for studying soils in a high vacuum and at high temperatures is to determine the engineering behavior of a particulate system with clean, dry surfaces. Once the properties have been established for clean surfaces, various degrees of "non-cleanliness" can be introduced to help determine the cause and the nature of friction between soil particles.

The relationship between the coefficient of friction, μ , of the solid surface and the Mohr-Coulomb angle of friction, ϕ_f , has been studied by many investigators including Caquot (1934), Bishop (1954), Newland and Allely (1957), and Rowe (1962). Rowe (1962) summarizes the previous work, and relates the dilatancy and strength of an assembly of particles to the angle of friction between the particle surfaces, $\phi_\mu = \tan^{-1} \mu$; the geometrical angle of packing, α ; and the energy expended during

shear due to volume changes.

The magnitude of ϕ_μ for various soil minerals has not received much study. The only comprehensive investigation to date is that by Horn (1961, also Horn and Deere, 1962). Clearly further investigation of ϕ_μ is required for a fundamental understanding of the strength behavior of soils, since ϕ_μ is the basic cause of the shear strength of granular soils.

The value of ϕ_μ has been shown to vary with the chemical composition of the solid, the surface topography, the type and amount of material adsorbed on the surface, and the conditions under which the tests are run. Each of these factors must be considered. A good point of departure is to consider the techniques and equipment required to produce an initially clean surface. The clean surface can be used as a point of reference for studying the effects of various changes in surface properties on the friction between surfaces, and thus on the strength of a granular mass.

II. THE USE OF HIGH VACUUM TO STUDY SURFACE PHENOMENA.

A. Introduction

Minute amounts of contamination, far below the level of chemical detection, may greatly affect the friction and adhesion of solid surfaces. Surfaces which are exposed to the atmosphere rapidly become contaminated with atmospheric gases, dust, and high molecular weight organic compounds. Friction and adhesion measurements on such surfaces, while useful for predicting normal behavior, are very difficult to interpret due to the poorly defined surface conditions.

A fundamental investigation of friction, therefore, requires an initially clean surface, free of any adsorbed contaminants, which is used as a standard reference point. To produce and maintain a clean surface requires a high vacuum, because at atmospheric pressure about 10^8 molecules per second impinge on every surface atom of the solid, resulting in very rapid contamination. Even if the atmospheric organic contamination is less than 1 part per million, a complete organic monolayer can form in a matter of seconds.

The length of time required for an initially clean surface to become covered with a monolayer of gas at various pressures can be calculated and used as a measure of the vacuum level necessary to maintain a clean surface. The following simplified analysis will be refined in Chapter IV and is only presented here to provide an illustration of the necessity of using low pressures.

The time for monolayer adsorption, t_m , may be calculated from the kinetic theory of gases:

$$t_m = \frac{1}{\sigma s Z} \quad 2.1$$

where σ is the area occupied per molecule ($\frac{1}{\sigma}$ is the number of molecules per square centimeter in a monomolecular layer), s is the sticking coefficient, i.e., the fraction of molecules striking the surface which remain on it, and Z is the number of molecules striking a square centimeter of surface per second. Fig. II-1 shows the time for monolayer formation plotted as a function of the gas pressure. The value of s used was 1.0, which is a reasonable value for adsorption on a high energy surface such as a clean metal where actual chemical bonding between the adsorbing gas and the surface occurs.

If the purpose of an experiment is to measure the properties of such a surface free of any contaminant films, and the time for the experiment is several minutes or hours, then the surfaces must be prepared and maintained in a vacuum of around 10^{-10} torr.

A pressure of 10^{-10} torr corresponds to 3.24×10^6 molecules/cc at 25°C . At this concentration the mean free path of a molecule, λ , is about 300 miles (λ in cm. is approximately equal to $5 \times 10^{-3}/p$, where p is in mm. of Hg.).

B. Preparing Clean Surfaces

The ultimate pressure of a vacuum system, P_u , is determined by the following equation:

$$P_u = \frac{Q_t}{S} \quad 2.2$$

where Q_t is the total influx of gas into the system, in torr-liters/sec*, and S is the speed of the pump in liters/sec. at the pressure P_u .

* The torr is the standard unit in vacuum technology and is equal to 1 mm. Hg.

The production of ultra-high vacuum is a matter of reducing the ratio of gas influx to pumping speed. This can be done by either increasing the pumping speed for a given system or by reducing the gas inflow. If a clean vacuum is desired, it is more reasonable to reduce the gas flow than to increase the pumping speed. Furthermore, although pumps can be obtained with speeds varying from a fraction of a liter per second to tens of thousands of liters per second, the price and size of a pump increase as the pumping speed increases. The optimum size pump for a laboratory system is generally less than 1000 liters/sec.

An average value for the total gas load, Q_t , for an unbaked vacuum system with rubber O-ring seals is about 10^{-4} torr-liters/sec. If this system were to reach $P_u = 10^{-10}$ torr, a pumping speed of 10^6 liters/sec. would be required. On the other hand, if the system could be redesigned so that the gas influx were 10^{-10} torr-liters/sec., then a miniature 1 liter/sec. pump would provide adequate pumping to reach 10^{-10} torr.

The gas influx is due to four sources:

- 1) leaks in the system welds, gaskets, etc.
- 2) backstreaming of gases from the pump.
- 3) desorption of gases from surfaces within the system.
- 4) permeation of gases through the walls of the system.

Items 1 through 3 can (and must) be reduced by careful system design. The magnitude of gas load due to each of these and methods for reducing them will be briefly considered. The level of vacuum technology which will be considered is that necessary to produce a vacuum of about 1×10^{-10} torr. This is an order of magnitude more difficult than producing a vacuum of 10^{-6} to 10^{-8} torr, but at least an order of magnitude simpler than producing a vacuum of 10^{-12} to 10^{-14} torr. Below 10^{-11} torr, permeation of gases through the walls may become important. Also, outgassing from hot tungsten filaments used as cathodes in pressure measuring gauges may cause a consid-

erable gas load. Ion pumps, which use a cold-cathode discharge, will probably extinguish and not pump at these pressure. The special problems involved in attaining pressures below 10^{-11} torr have been discussed by Davis (1962) and Roberts and Vanderslice (1963), and will not be considered here.

Leaks in the System

Leaks must be completely eliminated to attain ultra-high vacuum. A leak which consumes only 0.1% of the pumping speed at 10^{-7} torr and can be ignored in this range will consume the entire pumping capacity at 10^{-10} torr. The amount of gas inflow through a microscopic leak can be computed and related to the pumping speed necessary to remove this gas and thus attain a desired ultimate pressure. Fig.II-2 shows this relationship for a 1 micron diameter hole. Even if no other gas load existed in the system, pressures below 10^{-9} torr could not be obtained with such a leak.

Eliminating leaks is an essential part of high vacuum technology. Careful welding procedures, careful handling of all parts to prevent scratches or nicks, and use of knife-edge sealed metal gaskets will give a system with no detectable leaks larger than 10^{-10} std.cc./sec. A leak of 10^{-10} std.cc./sec. will only consume about 1 liter/sec. of the pumping speed at 10^{-10} torr.

Apart from actual leaks to the atmosphere, care must be taken to minimize so-called virtual leaks, which are due to small pockets of trapped air or contamination. These leaks arise from poorly welded joints which entrap air and from improperly cleaned materials. They are difficult to detect, the only evidence for their existence being the failure of the system to reach low pressures.

A small pocket of gas which raised the pressure of a vacuum chamber at 10^{-6} torr by 1%, would raise the pressure at 10^{-10} torr by 10,000%, perhaps contaminating a test surface and ruining an experiment. Virtual leaks often release their gas slowly, causing

a system to remain at 10^{-6} to 10^{-8} torr for days or months.

Virtual leaks can be minimized by careful welding, always welding on the vacuum side to prevent cracks or crevices; careful cleaning of all materials exposed to the vacuum; and elimination of all high vapor pressure materials.

Backstreaming of Gases From the Pump

Both ion pumps and diffusion pumps, the two major methods for obtaining a high vacuum, are sources of gas. Diffusion pumps, which utilize a vaporizable fluid, are likely to contaminate the system with this fluid. Backstreaming in diffusion pumps is reduced by placing a cold surface between the pump and the chamber which will trap and condense the backstreaming molecules. The effectiveness of this trap (or usually a series of traps) determines the cleanliness of the vacuum.

Ion pumps are less susceptible to backstreaming, but can release appreciable amounts of low molecular weight materials, particularly H_2 , H_e , and CH_4 , into the system if they are not operated properly. Generally speaking, ion pumps provide a very clean vacuum without the use of elaborate and costly trapping devices.

Cryogenic pumping, using liquid helium cooled surfaces to trap and condense gases, is most nearly an ideal pump into which a molecule goes and never returns to the chamber. Only helium and hydrogen have appreciable vapor pressures at liquid helium temperature ($4^{\circ}K$). These gases are usually removed by an auxiliary diffusion pump or ion pump. Cryogenic pumping is a means for obtaining an essentially perfect vacuum. Calculations by J. P. Hobson (Holland, 1964, p. 265) indicate that if a Pyrex bulb was pumped down to 5×10^{-10} torr of helium gas and then immersed in liquid helium, the pressure would fall to 10^{-32} torr. The bulb would thus contain a free molecule for about 1 second out of every 10,000 years.

Desorption of Gases Within the System

Any surface which has been exposed to the atmosphere is contaminated by adsorbed gases. The ease with which gases can be removed depends upon how tightly they are held, i.e., the adsorption energy. Physically adsorbed water can be removed by slight warming at pressures around 10^{-3} torr. Chemically adsorbed oxides, on the other hand, may require heating to 2000°C . at 10^{-9} torr. The thermodynamics of desorption will be considered in more detail in Chapter IV. However, the importance of minimizing outgassing within the system can be easily shown.

At 10^{-10} torr, there are about 3×10^6 molecules in each cubic centimeter of space within a vacuum chamber. On each square centimeter which is covered with a monolayer of gas, however, there are about 10^{15} molecules. Even if the adsorbed gas is reduced to 10^{-6} of a monolayer, there will still be several hundred times as much gas on the surface as in the volume of the system at 10^{-10} torr.

The rate of desorption can be decreased by cooling the walls of the vacuum chamber. Generally it is more practical to heat the chamber walls, increasing the rate of desorption and driving off most of the adsorbed gas, which is removed from the system by the pump. By this means, the outgassing of stainless steel can be reduced from an initial value of about 10^{-8} torr-liter/sec/cm² to less than 10^{-14} torr-liter/sec/cm².

Permeation Through the System Walls

The permeation of gases through the walls of the chamber determines the ultimate pressure of a system which has no leaks and no adsorbed gases on the interior walls. The permeability of Pyrex glass to helium is about 10^{-12} torr-liters/sec/cm² surface, and stainless steel to hydrogen is about 10^{-14} torr-liters/sec/cm² (per mm of thickness). Therefore permeability will be a major problem at pressures below 10^{-12} torr, but will generally be of little

importance at 10^{-10} torr and higher.

C. The Degree of Cleanliness of a Vacuum

The pressure of a vacuum system is an inadequate measure of its suitability for maintaining a clean surface. Because the time required to pump a system down and to complete a test may be several days or even weeks, the types of gases which make up the vapor phase are as important as the pressure level.

Consider, for example, an inadequately trapped diffusion pump using the lowest vapor pressure pump fluid available (DC705 with a room temperature vapor pressure of less than 1×10^{-9} torr). Although the pressure of this system will remain in the 10^{-10} torr range, in a matter of hours a monolayer of oil will have covered everything within the system, and the layer will continue to grow at a rate of about $5 \text{ \AA}^0/\text{hour}$ (Holland, 1964, p. 343).

If the total pressure is 10^{-6} torr, however, and the only gas present is helium, this may be considered a very clean vacuum, because helium has a very low adsorption energy and will not contaminate a surface at this pressure.

In most cases, it is advantageous to know the gas composition in the system since the residual gas may vary with different materials, temperature, and time. Residual gas analysis requires a mass spectrometer tube which is capable of measuring partial pressures down to about 10^{-12} torr if the system total pressure is 10^{-10} torr. Such units are commercially available for about \$10,000.

A variety of techniques may be used to estimate the cleanliness of a vacuum in lieu of a mass spectrometer, but all of them involve various degrees of uncertainty because the actual gas composition is not measured.

Wettability of Clean Surfaces

A very simple and sensitive test utilizes the spreading of water on a clean metal or glass surface. A drop of water placed on a

clean surface will rapidly spread and show a low contact angle because of the strong adhesive forces at the solid surface. If, however, a minute amount of organic contaminant is present, the drop of water will not wet the surface. High vacuum experiments for which clean surfaces are claimed should, as a minimum, corroborate this assumption by placing an initially clean, wettable strip of metal in the test chamber and checking its wettability at the end of the experiment.

Unfortunately, this test is not sufficiently sensitive to ensure clean surfaces. The surface energy of a clean metal surface can decrease appreciably (by adsorption of O_2 , CO_2 , H_2O , etc.) and still be high enough to cause a drop of water to spread. But it remains a good test for gross contamination.

Flushing With a Rare Gas

An effective but seldom employed method of reducing the undesirable gaseous components in a high vacuum system is to leak a less undesirable gas such as helium into the system at constant pressure. As the pump continues to remove gas from the system, the partial pressure of the undesirable gases will be lowered until essentially all of the gas present is helium. The mathematics of the flushing procedure were first presented by H. Belofsky (1962) and are described, with slight modification, in Appendix I.

By evacuating a vacuum chamber to 1×10^{-8} torr, baking to desorb the walls, and at constant pressure flushing through an amount of helium (containing no more than 2 ppm of other gases) equivalent to 10 volumes of the chamber, and then pumping down to 1×10^{-10} torr, the pressure of all the gases other than helium will be less than 1×10^{-14} torr. Such a low pressure of offensive gases would ensure a clean surface for almost a year.

Care must be taken that impurities are not admitted along with the pure gas. Young and Whetten (1961) found that impurities amounting

to 30 ppm of CO and 10 ppm of H₂ were admitted along with the pure gas, presumably due to the method of admitting the gas. This level of contamination, for the example given above, would result in partial pressures due to impurities of about 6×10^{-13} torr, which is still an exceptionally clean vacuum.

The most effective method of admitting gases is through a selective semipermeable membrane which is highly specific as to gas and results in the admission of a gas of very high purity. Such inlets contain no moving parts and can be readily attached to bakeable vacuum systems. (Roberts and Vanderslice, 1963).

Friction as a Measure of Surface Cleanliness

Friction can be a very sensitive measure of surface contamination. If a friction test is run in a high vacuum on a material such as glass which, if clean, would have a μ of about 1.0, the actual value of μ can be used as a measure of the amount of contamination which occurred. Holland (1964, p. 302ff) reports that glass cleaned with a detergent gave a coefficient of friction of 0.07. If it was then placed in a vacuum, baked, and bombarded with positive ions (glow discharge cleaning) the friction coefficient increased to 0.9.

Changes in μ due to contamination from diffusion pump fluid (DC704) were also measured by Holland (1964, p. 340ff). Glass cleaned with detergent and alcohol and giving an initial $\mu = 0.3$ was placed in a vacuum chamber. If the sample was then glow discharge cleaned, μ increased to 0.85 and maintained this value for extended bombardment times, as shown in Fig. II-3. If, however, the discharge was stopped and the temperature raised to 230°C, μ quickly dropped to 0.45. Another sample was placed in the vacuum and μ measured vs. time with no glow discharge cleaning. The friction initially increased to 0.55, then decreased as silicone oil was chemisorbed until after one hour it was lower than the initial value.

D. Conclusions

The study of friction and adhesion of clean surfaces requires temperatures of 200° to 500° C and pressures of 10^{-10} torr. The pressure level is not an adequate measure of the ability of the vacuum to maintain a clean surface because contamination can occur even at 10^{-10} torr. Knowledge of the composition of the gas is very useful and may be required to adequately interpret experimental results. When spectroscopic analysis is not possible, other techniques such as wettability, purging of offensive gases, and friction measurements should be used to indicate the cleanliness of the vacuum.

Monolayer Formation Time vs. Pressure

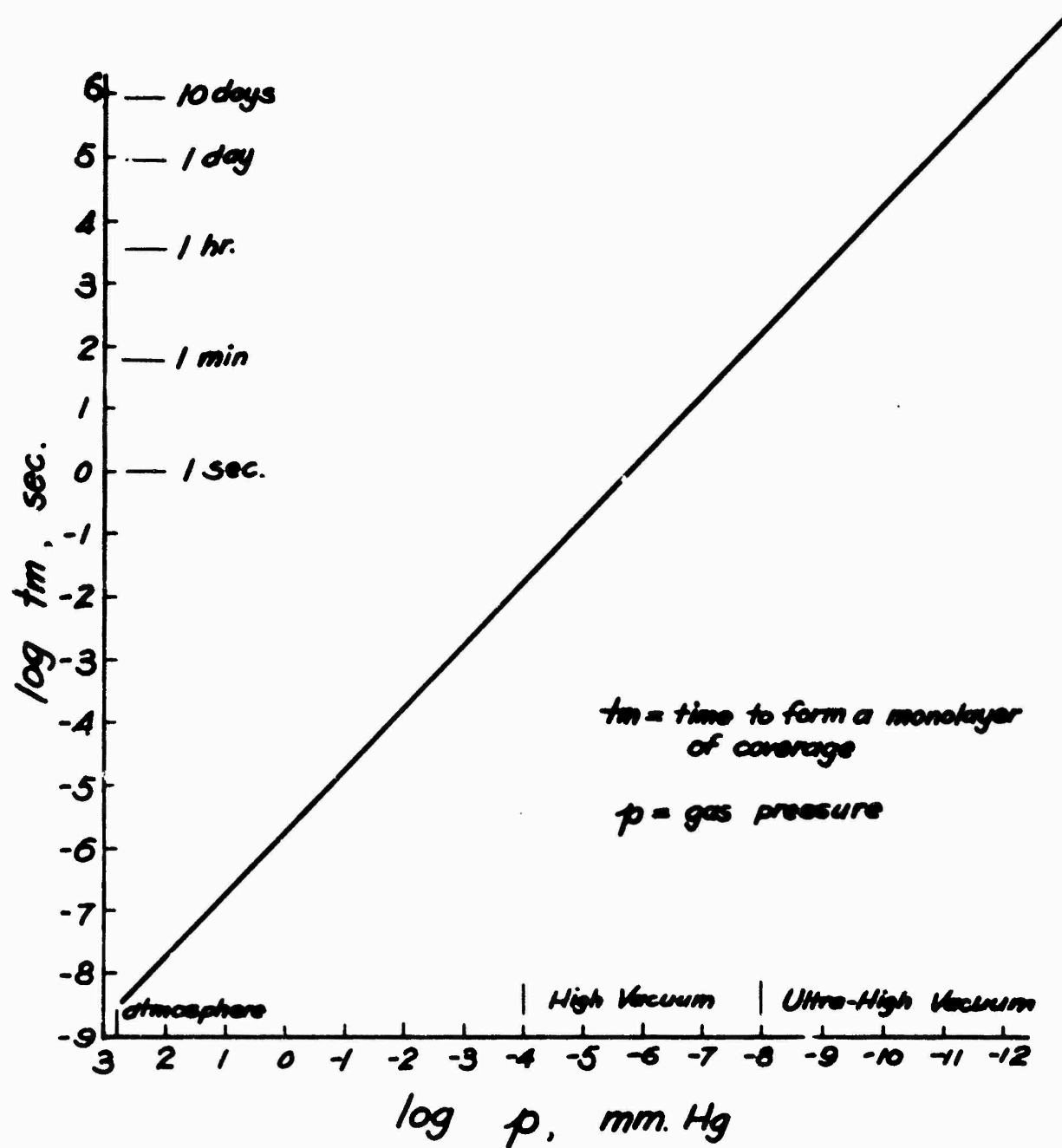


Figure II-1

Ultimate Pressure vs. Pumping Speed

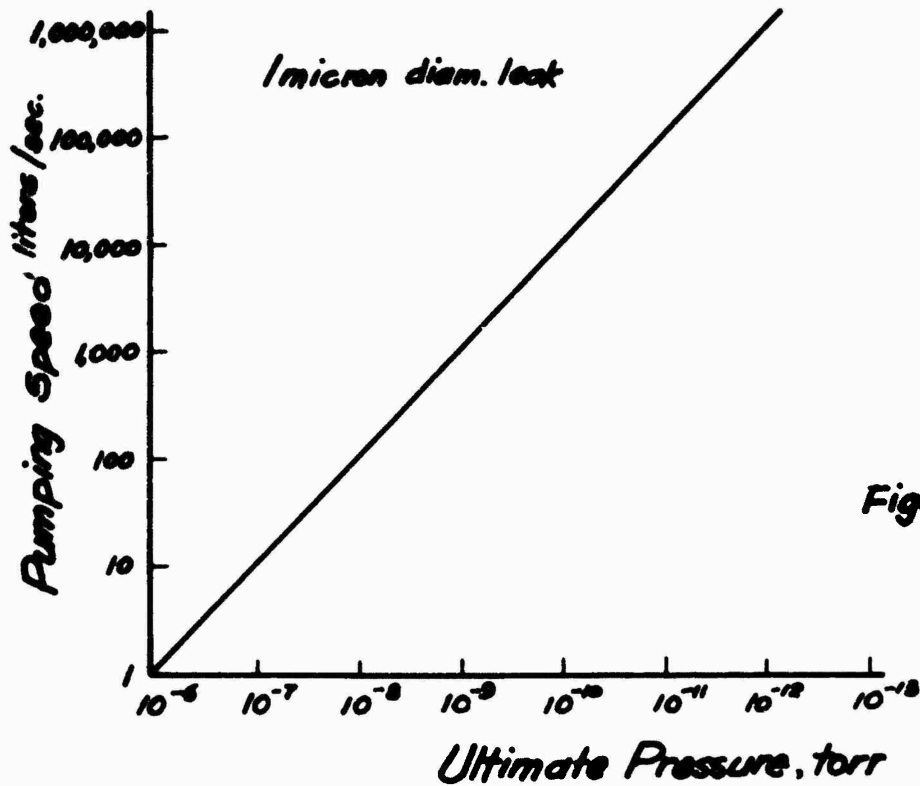


Figure II-2

Contamination of Glass by Diffusion Pump Oil (from Holland, 1964)

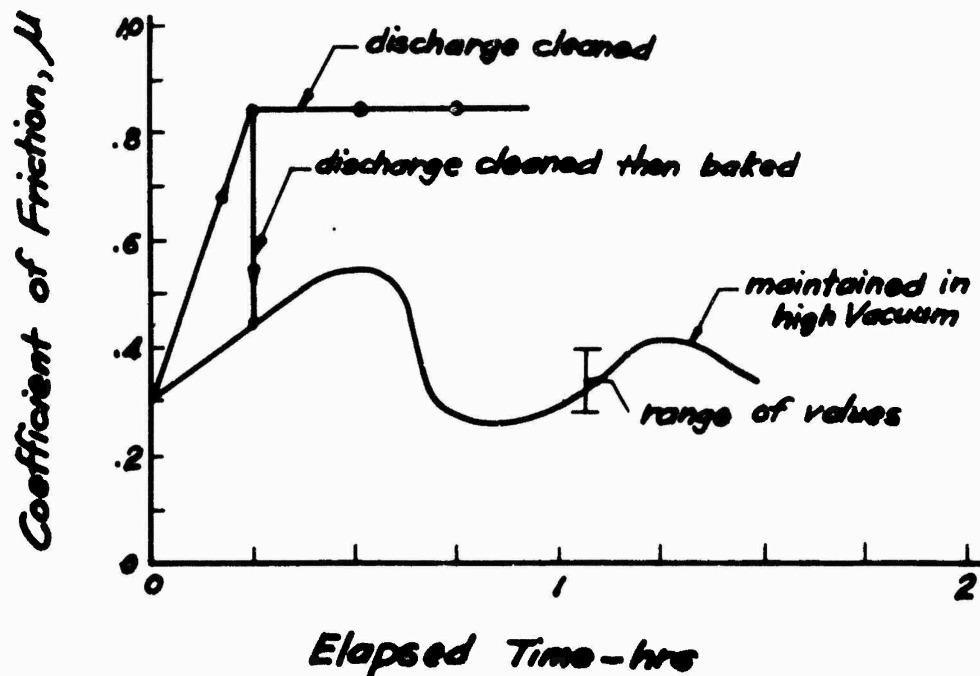


Figure II-3

III. THE SOLID SURFACE

A. Nature of the Solid Surface

Roughness of Surfaces

A major difficulty in studying the surfaces of solids is that, with few exceptions, they are extremely rough on a molecular scale.* Even a carefully polished surface consists of hill (called asperities) and depressions which generally range from 100 Å to 1000 Å high. An accurate representation of a metal surface ground to an 8 micro-inch (root mean square) finish (2000 Å) is shown in Fig. III-1. This drawing is reproduced from an actual measured surface profile (Sonntag, 1961). The slopes, which were found to vary between 128° and 172°, are quite gentle compared with many imaginary hand-drawn portrayals of surfaces, which often show almost vertical slopes. The American Standards Association, after checking surfaces of various metals over a large range of roughness, reached the conclusion that the average slope of asperities is an included angle of 150°.

Metal surfaces can be produced with an average roughness of about 1 micro-inch or 250 Å. When two such surfaces are in contact, they still will be supported on the summits of the highest asperities, and the actual area of contact will be a small fraction of the apparent area. This has a profound influence on the friction and adhesion between the surfaces, as will be shown in Chapter V.

The necessity for very smooth surfaces for optics has resulted in a large amount of work on the polishing of glass. For light reflec-

* A commonly used base for a molecular scale is the angstrom(Å):

$1 \text{ Å} = 10^{-8} \text{ cm}$
 $1 \text{ micron} = 10^{-4} \text{ cm} = 10,000 \text{ Å}$
 $1 \text{ micro-inch} = 10^{-6} \text{ inch} = 254 \text{ Å}$

tion, surface irregularities should be less than $\lambda/16$, where λ is the wavelength of the incident light (Holland, 1964, p.76). For blue light, this permits asperities of about 250 Å.

Extremely smooth glass surfaces can be prepared, but they are difficult to maintain. The root mean square height of two fire-polished microscope slides in contact was measured by multiple-beam interferometry as 56 Å (Holland, 1964, p. 119). Rapid erosion occurs if such surfaces are left in contact with the atmosphere. The hygroscopic alkali oxides (NaO, CaO) in the glass absorb water vapor, and the resulting high pH solution attacks the silica causing erosion pits.

Common washing techniques, such as chromic acid cleaning solution, can greatly increase the surface area and surface roughness of glass. The surface area of glass beads as measured by CO₂ adsorption was increased by a factor of 10 or more when the beads were immersed in water for 33 days (J.B. Thompson, et. al., 1952). No satisfactory method for producing and maintaining very smooth glass surfaces (less than 250 Å) has been reported.

Extremely smooth surfaces can be produced by cleaving mica. Steps ranging between 10 Å and 1000 Å normally result when mica is cleaved, but by taking extreme care, molecularly smooth cleavage faces can be produced (Bailey and Courtney-Pratt, 1955). These smooth faces have been used for fundamental investigations on friction, adhesion, adsorption, and surface energy. The results will be discussed in the sections of this report dealing with these various topics.

Even the cleavage face of muscovite has been shown to be wavy on an atomic scale (a few tenths of an angstrom) due to rotation of the tetrahedra in the silica layer. The effect of this small-scale waviness on various surface properties has not been investigated.

Surface Structure

When a crystal is broken the surface atoms have fewer nearest neighbors than the atoms in the bulk of the solid. Because of the fewer bonds, these atoms are less restrained and hence at a higher energy level. The drive to decrease the difference in free energy (called the surface energy) between the atoms in the bulk and the surface atoms is the fundamental explanation for all of the phenomena considered in this report. The surface energy of a solid can be reduced by either decreasing the surface area (by adhesion to another surface) or by lowering the energy of the individual surface atoms (by adsorption or by surface rearrangement).

When a quartz surface is broken, two kinds of surface sites are formed; one terminating in an oxygen ion with an excess of electrons and a negative charge, the other in a silicon ion with a deficiency of electrons and a positive charge. The oxygen ions, being larger and more polarizable, probably shield the smaller silicon ions. For example, the distance between the outer and second layer in NaCl is 2.66 \AA for $\overset{\text{O}}{\text{Na}^+}$ and 2.86 \AA for $\overset{\text{O}}{\text{Cl}^-}$, producing a field which will predominantly attract a positive charge (Gregg, 1961, p. 17). The same might be expected to occur for SiO_2 , except that rapid adsorption of H_2O usually occurs on quartz, the H^+ going to the O^- site and the OH^- to the Si^+ site, producing a hydrated Si-OH surface.

Because the surface atoms of solids are essentially immobile under normal conditions, the structure of the surface depends greatly on the previous treatment and environment. Chemical alteration of glass surfaces, which has been briefly discussed, is an example of this. Further evidence comes from the effects of grinding and polishing on surface structure.

Grinding requires a material as hard or harder than the surface to be abraded. If the grinding material is appreciably harder, mechanical attrition of the surface will result without greatly

changing its crystallinity. However, measurements of transfer of tool material during cutting operations (Bowden and Tabor, 1964, p. 108) indicates that about 10^{14} atoms of the grinding material may be transferred to each square centimeter of solid surface. This is the order of magnitude of atoms required to give monomolecular surface coverage, and thus may represent appreciable surface contamination.

Polishing materials are often softer than the surface to be polished but have a higher melting point. The polishing operation results in local melting at points of contact due to frictional heating, followed by smearing of the melted material over the surface. This normally results in a fairly deep amorphous layer, with large amounts of entrapped impurities. The amorphous layer can be removed by chemically etching the surface, but this also destroys the smoothness.

Grinding of quartz has been shown to produce an amorphous surface layer (Dempster and Ritchie, 1953). A quartz sand (99.9% SiO_2) was ground in an agate mortar for 17 hours, after which it was shown by DTA to have only 1% crystalline quartz. The thickness of the disturbed layer was calculated to be 0.15 micron or 1500 \AA . Etching with hydrofluoric acid restored the quartz content to 100%. The etching tests indicated a highly disturbed and very soluble surface layer about 0.03 micron thick (300 \AA). Estimates of a layer with some disturbance as deep as 100 microns have been made for quartz (Iler, 1955, p. 259).

A schematic drawing of a polished quartz surface is shown in Fig. III-2. Deviations from ideality include surface roughness, adsorbed contaminants, and an amorphous surface layer.

B. Surface Forces and Surface Energy

The Nature of Surface Forces

When a solid is cleaved or broken, the instantaneous force field

existing at the surface will be of the same character as the forces which hold the atoms in the solid. These forces are generally divided into two categories: primary valence forces, which are generally of the order 10-100 Kcal/gm.mole, and secondary valence forces, which are generally much less than 10 Kcal/gm.mole, but in some cases are as strong as weak primary bonds. Both primary and secondary forces are a result of the charged nature of the electron cloud surrounding atoms, and therefore differ in degree, rather than kind. Primary valence bonds usually involve large electron displacements, resulting in charged atoms when the bonds are broken. Examples of such bonds are metallic, covalent, and ionic chemical bonds.

There are three types of secondary valence bonds: orientation, induction, and dispersion. Interactions between permanent dipoles cause the orientation effect. Permanent dipoles also induce charge separations in molecules which normally have no dipole moment and induction bonds result. Dispersion bonds are thought to arise from the fluctuating electromagnetic radiation of the electron cloud, and do not require large electron displacements nor a permanent separation of charge. The dispersion forces are a universal property of matter and hence always act. Their contribution to the total energy of a given system may be negligible or they may be the main contribution, as in the case of solidification of the inert gases.

In principle it should be possible to calculate the field of force at the solid surface. Except for a few cases, however, this has not been done for atom-atom interactions leading to primary valency bonds. This is largely due to insufficient theoretical development of quantum mechanics and statistical methods which would permit a complete description of the energy states of the surface atoms. Secondary valence interactions, due to so-called van der Waals forces, have been largely worked out (Verwey and Overbeck, 1948), but conclusive experimental verification of the equations is still lacking. For purposes of this report, a more convenient measure

of the forces acting at the solid surface is the surface energy.

The Surface Energy of Solids

The surface energy of solids is much more amenable to analysis and experimental determination than are surface fields of force. Values of surface energy can be used to predict and to interpret the amount of adhesion between solids and the amount of adsorption on solid surfaces.

The surface free energy of a solid is the isothermal reversible work expended in creating 1 cm^2 of new surface. A diagrammatic representation of an imaginary experiment measuring the surface energy is shown in Fig. III-3. An elastic solid of 0.5 cm^2 cross-section is slowly pulled apart in a vacuum, producing two new surfaces with a total area of 1 cm^2 , and requiring an amount of work equal to γ_0 . If the two pieces are now put back into contact, the energy gain will be γ_0 and they will readhere. If, however, a gas is allowed to adsorb on the broken surfaces, the intensity of the surface force field of the solid will decrease. Hence the surface energy will be reduced to a value γ_v . The change in surface energy, $\gamma_0 - \gamma_v$, can be determined by the Gibbs adsorption equation, which will be discussed in Chapter IV. If the contaminated surfaces are put back into contact, the energy gain will be γ_v and they will not readhere as strongly.

In practice, surface energies are rarely easy to measure for solids. Unless the measurements are made in an ultra-high vacuum, the values obtained may represent γ_v rather than γ_0 . Measured values for glass range from about 190 ergs/cm^2 (from the heat of wetting), to 1200 ergs/cm^2 (cleavage of a glass plate). Brace and Walsh (1962) measured the surface energy of quartz and orthoclase. They obtained values ranging from 410 to 1030 ergs/cm^2 for quartz (depending on the cleavage direction) and 7770 ergs/cm^2 on the (001) cleavage plane of orthoclase. They also give references to other determinations of surface energies for minerals. Many investigators

have measured the surface energy of mica as about 300 ergs/cm² in air. Bryant (1962), using a vacuum of 10⁻¹³ torr, obtained 5125 ergs/cm², illustrating the importance of maintaining clean surfaces.

Using an ideal crystal lattice model, Michaels (1962) has calculated the work necessary to bring a bulk atom to the surface. The resulting relationship for surface free energy is as follows:

$$\gamma = \left(1 - \frac{n_s}{n}\right) \frac{\Delta E_{\text{vap}}}{N^{1/3} (M/\rho)^{2/3}} \quad (3.1)$$

where

ΔE_{vap} = heat of vaporization, ergs/mole

n_s = number of nearest neighbors for a surface atom

n = number of nearest neighbors for a bulk atom

$N = 6.02 \times 10^{23}$ molecules/mole

M = molecular weight, gm/mole

ρ = density, gm/cm³

Although this formula is most often used for liquids, the model used is more closely approximated by a crystalline solid. It should give a reasonable estimate of the surface energy of elemental solids, but may not be accurate for complex crystals. Values of surface energy for diamond and quartz calculated by this formula are given in Table III-1, along with experimental values and values calculated by other theoretical methods to be described.

Theoretical calculations of surface energy can be made by considering the bonds broken during cleavage. The surface energy γ_0 , is taken as $\frac{1}{2}$ the energy required to rupture the number of bonds passing through 1 cm² (two cm² of surface are produced for each cm² of bonds broken). This calculation actually gives the total surface energy, E_s , and the free surface energy, γ_0 , is related to the total surface energy by

$$E_s = \gamma_0 - T \frac{\delta \gamma}{\delta T} \quad (3.2)$$

but for most solids around room temperature $\frac{\delta \gamma}{\delta T}$ is small, and E_s may be taken as γ_0 (T = absolute temperature).

For diamond, with 1.83×10^{15} bonds/cm² on the close-packed (111) plane and a bond energy of 83 Kcal/mole, the calculated value of γ_0 is 5400 ergs/cm². On the (100) plane, where two bonds must be broken for each carbon atom, γ_0 is 9000 ergs/cm² (Adamson, 1960, p.238).

In a similar manner, surface energies for quartz may be calculated. Iler (1955, p.108) gives a value of 2 bonds/23.4 Å² of quartz surface, which leads to 8.6×10^{14} bonds/cm². Pauling (1960, p.85) gives the bond energy of the Si-O bond as 88.2 Kcal/mole, or 3.7×10^{12} ergs/mole of bonds. Therefore, the theoretical surface energy is

$$\begin{aligned}\gamma_0 &= 1/2 (8.6 \times 10^{14}) (3.7 \times 10^{12}) \left(\frac{1}{6.02 \times 10^{23}} \right) \\ &= 2640 \text{ ergs/cm}^2\end{aligned}$$

The surface energy values from hardness measurements shown in Table III-1 are calculated from a correlation by Rabinowicz (1961), who found that for most metals a plot of surface energy vs. hardness on a log-log scale fell reasonably close to a straight line with a slope of $\frac{1}{4}$. Minerals fell near a line parallel to that for metals, but lower, indicating smaller values of surface energy for the same value of hardness. This correlation is rough and should only be used to indicate an order of magnitude.

The wide range of surface energy values shown in Table III-1 for quartz (260 to 3100) and mica (300 to 5100) illustrate the problems involved in making these measurements and in using the data for theoretical calculations of surface forces and bonding energies. The low values are obtained on contaminated surfaces where the surface energy clearly is not that of the clean solid, γ_0 . If the surfaces are maintained clean and molecular rearrangements do not occur, the upper values should be applicable.

Surface energy values are a measure of the adhesive forces which may be brought into play when two surfaces are touching. Thus, clean surfaces of diamond, quartz, and mica may be expected to adhere strongly at the points of contact. The magnitude of the surface energy is not the only consideration in determining the amount of adhesion between solids, however, unless the surfaces are molecularly smooth and contact can occur over the entire area. This point will be discussed more completely in Chapter V.

Table III-1 Measured and Theoretical Values of Surface Energy

<u>Material</u>	<u>Surface Energy (ergs/cm²)</u>		<u>Method</u>	<u>Reference</u>
	<u>Measured</u>	<u>Theoretical</u>		
Quartz	410		cleavage (10 $\bar{1}$ 1) plane	Brace and Walsh (1962)
	1030		cleavage (10 $\bar{1}$ 0) plane	Brace and Walsh (1962)
		480-760	from elastic constants	Brace and Walsh (1962)
	260		from heat of wetting	Gregg (1961)
		600	from hardness	
		3100 2640	from ΔE vap from crystal structure	
Orthoclase	7770		cleavage (001)	Brace and Walsh (1962)
		200	from elastic constants	Brace and Walsh (1962)
		500	from hardness	
Glass	190		from heat of wetting	Gregg (1961)
	540		crack propagation	Griffith (1920)
	1210		crack propagation	Gregg (1961)
Mica	300		cleavage in air	Bailey and Courtney-Pratt (1955)
	5100		cleavage in vacuum	Bryant (1962)
Diamond		5400	from crystal structure(111) plane	Adamson (1960)
		9000	from crystal structure (100) plane	Adamson (1960)
		9100	from ΔE vap	
		1300	from hardness	

*Contact Between Two Smooth Surfaces
(from Sonntag, 1961)*

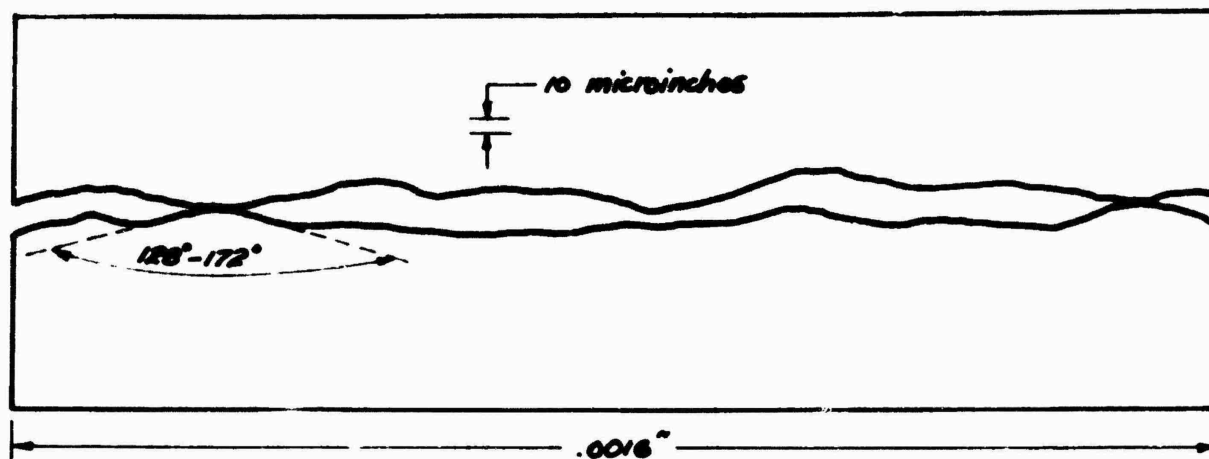


Figure III-1

Surface Structure of a Polished Crystalline Solid

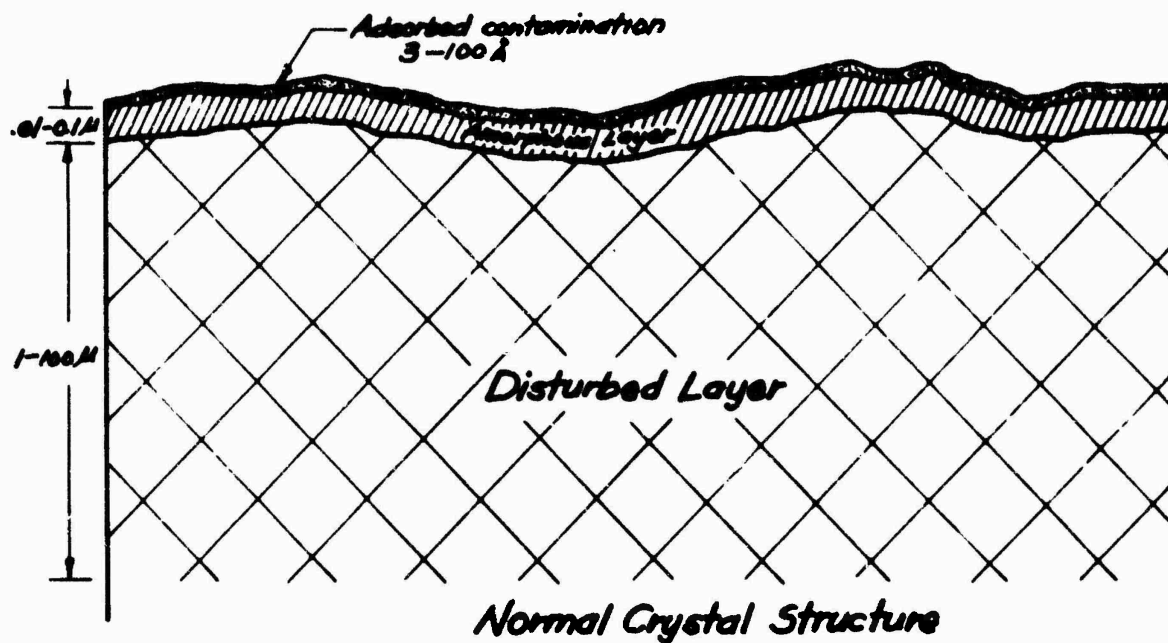
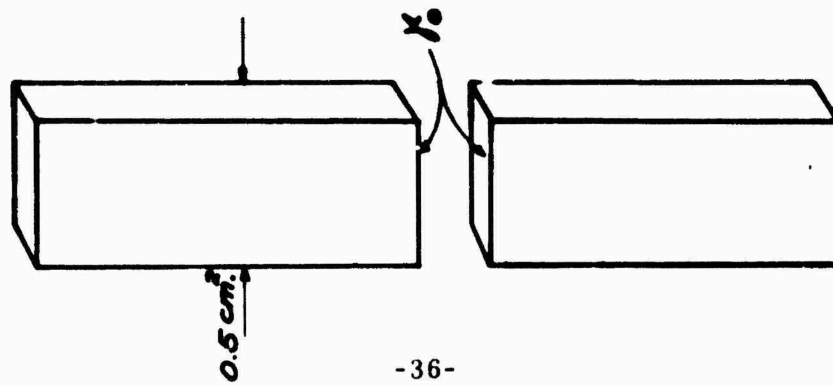


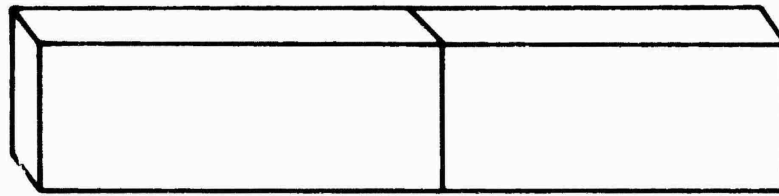
Figure III-2

The Surface Energy of Solids



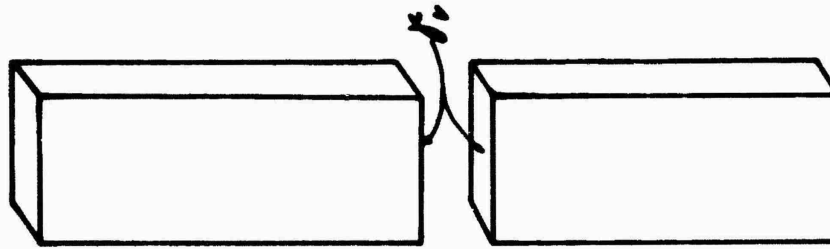
(a)

Work input = γ_0



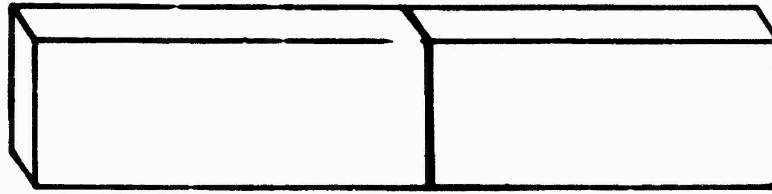
(b)

Energy gain = γ_0



(c)

Surfaces Contaminated
Energy Reduction = $\gamma_0 - \gamma_1$



(d)

Energy gain = γ_1

Figure III -3

IV. ADSORPTION ON SOLID SURFACES

The existence of contaminating films on all solid surfaces exposed to the atmosphere was pointed out in Chapters II and III. This chapter will consider the nature of these films and the forces which bond them to the solid. This information will aid in understanding the friction between contaminated solid surfaces, which is discussed in the next chapter. Furthermore, it will help in understanding the conditions required to remove the contamination and produce a clean surface.

A. Atomic Forces and Adsorption

The trajectory of a free gas molecule impinging on a solid surface will be altered by the interaction of the force field of the gas molecule with that of the surface atoms of the solid. During the time of this interaction the gas is considered to be adsorbed on the surface. An equation relating the time of adsorption, τ , to the adsorption energy Q , was derived by J. Frenkel (Adamson, 1960, p. 461):

$$\tau = \tau_0 \exp (Q/RT) \quad (4.1)$$

where $\tau_0 \approx 10^{-13}$ sec = time for a specular reflection

R = perfect gas constant = 1.98 cal/mole $^{\circ}\text{K}$

T = absolute temperature, $^{\circ}\text{K}$

Calculated values of the average time of residence for various assumed values of Q are given in Table IV-1. For adsorption energies less than 10 Kcal/mole (physical adsorption), the times are very short -- less than 1 micro-second at room temperature. For large adsorption energies the times are extremely long, and equation 4.1 should be replaced by a more exact probability analysis. For example, the calculated residence time for oxygen on steel (about 30 Kcal/mole) is 300 years. This indicates formation of a chemical compound at the surface with a rather low vapor pressure. The upper limit of measured adsorption energies is 123 Kcal/mole for O_2 on tungsten.

Although it is often convenient to assign a single value to the adsorption energy for a given adsorbate-adsorbent system, the actual situation is much more complicated. The first molecules to arrive on a surface will tend to sorb on the most active surface sites (edges, corners, heights of asperities), with a corresponding large energy of adsorption. When these sites are filled, adsorption takes place on less active sites and the adsorption energy decreases. As the number of adsorbed molecules increases they begin to interact with each other, causing less favorable conditions for adsorption, and a further decrease in adsorption energy.

The energy of repulsion between like-oriented dipoles has been calculated as

$$U_{\text{int.}} = -\frac{\mu^2}{2r^3} \quad (4.2)$$

where μ is the dipole moment and r is the separation between charges. This repulsion is appreciable at distances up to 100 Å and has been used to explain decreasing adsorption energy with increasing surface coverage (Gregg, 1961, p. 93). After a monolayer has formed and the surface atoms of the solid are shielded, further adsorption, if it occurs, will be at a lower adsorption energy, approaching the heat of liquefaction of the adsorbate gas.

B. Surface Energy and Adsorption Energy

It seems intuitively reasonable that the energy of adsorption for a given adsorbate gas will increase as the surface energy of the solid increases. This is generally found to be true, although chemical bond formation sometimes alters the picture.

Covalent or partially covalent crystals, whose bonds are directional, can be visualized as having a surface composed of dangling bonds, consisting of empty, partially filled, or filled electron orbitals (Gatos, 1962). If an adsorbate atom or ion is able to donate or accept electrons as the case may require, a very strong bond may be expected to result.

The other extreme is an uncharged surface and an inert gas, with only van der Waals type interactions, and relatively weak bonds. Between these two cases lies a hazy area which encompasses many interesting actual systems, including most of those of interest to soil mechanics. Nevertheless, surface energy concepts, coupled with knowledge of the nature and types of chemical bonds, can greatly aid in interpreting and predicting the behavior of these systems.

The Gibbs Adsorption Equation

The Gibbs adsorption equation can be used to relate changes in surface free energy to the amount of adsorbed gas (Gregg, 1961, p.60). If γ_0 is the surface energy of the clean solid and $d\gamma$ the change in surface energy after an amount of gas Γ (moles/cm²) has been adsorbed at a gas pressure p and temperature T , then

$$-d\gamma = RT \Gamma d(\ln p) \quad (4.3)$$

Integration of equation 4.3 gives

$$(\gamma_0 - \gamma_v) = RT \int_0^p \Gamma d(\ln p) \quad (4.4)$$

where γ_v is the surface energy after adsorption. By integrating the area under the curve of Γ vs. $\ln p$ from zero pressure to pressure p , the change in surface energy can be found. Actual adsorption experiments usually measure the weight of a gas adsorbed, X_m , from which Γ can be calculated,

$$\Gamma = \frac{X_m}{MS} \quad (4.5)$$

where M is the molecular weight of the gas and S is the surface area of the solid.

For physical adsorption, values of $\gamma_0 - \gamma_v$ are commonly of the order of 100 ergs/cm². For chemisorption the change is much greater and the amount adsorbed, Γ , is essentially independent of the pressure if the adsorption energy is sufficiently high (above 25 Kcal. at room temperature). A clean tungsten surface will

eventually adsorb a monolayer of oxygen, even if the partial pressure of oxygen is 10^{-16} torr, due to the long residence time τ .

Chemisorption which involves large adsorption energies is a time controlled, rather than a pressure controlled phenomenon at room temperature. At increased temperatures, the residence time will be lower, and the Gibbs equation may be applied. This provides a means for studying the effect of changing surface energy on other surface properties, such as friction and cohesion. However, temperature variations may and probably will induce changes in surface properties which would be difficult to separate from surface energy changes per se. Therefore, the Gibbs equation will probably have limited application for clean surfaces.

C. The Nature of the Adsorbed Layer

The nature of the adsorbed layer (particularly its structure, thickness, and mobility) to a large extent determines the surface properties of the solid. Unfortunately, these items are very difficult to determine directly, and they are usually inferred from adsorption experiments on a contaminated, poorly defined surface.

The necessity for using clean reproducible surfaces in any study which attempts to interpret data in terms of a molecular model has been pointed out by Martin (1960). Martin's conclusions regarding the lack of incontrovertible data on clay-water systems may be applied to much of the available information on solid surfaces. Definite conclusions regarding the nature of the adsorbed layer can seldom be made. For this reason, much of the following discussion is qualitative.

The Structure of the Adsorbed Layer

For physically adsorbed molecules, various assumptions can be made. The adsorbate can be assumed to have the same structure as it normally has in either the liquid or solid state, or a close-packed structure can be assumed. The assumptions can be checked

by calculating the area occupied per molecule, which requires an independent measure of the surface area and knowledge of when the monolayer point is reached. This method is generally useful only for large organic adsorbates with a large effective area. Such molecules can be shown to be stacked upright on some surfaces (generally hydrophilic) and spread out on others (generally hydrophobic).

Molecules adsorbed on covalent crystals would be expected to have fixed locations on the surface corresponding to "dangling bond" sites. The density and location of the adsorbate molecules can be calculated from a knowledge of the crystal chemistry of the solid.

The ideal quartz surface, which has one anionic and one cationic site per 23.4 \AA^2 of surface is shown schematically in Fig. IV-1a. The surface is normally assumed to hydrate rapidly as in (b). This would require about 4×10^{14} water molecules/cm², which is a relatively loose surface packing. A close-packed water layer would require about 1.2×10^{15} water molecules/cm².

The quartz surface can be made hydrophobic by adding dimethyl chlorosilane as shown in (c). The resulting surface has a very low surface energy and should exhibit markedly different properties than the quartz surface.

The Thickness of the Adsorbed Layer

A chemically adsorbed layer is usually only one molecule deep. Two molecular layers of chemisorbed oxygen have been found on tungsten (Becker, 1958), with the second layer having about one-quarter of the adsorption energy of the first layer.

Physically adsorbed layers can be of any thickness depending on the partial pressure of the gas. At very low partial pressures, adsorption is generally limited to a fraction of a monolayer. As the partial pressure approaches the saturation pressure, multilayers can build up by bulk condensation on the surface.

Many attempts have been made to support the existence of multiple layers tightly bound to a solid surface by long-range forces. Various investigators from Faraday to Terzaghi have observed that two smooth surfaces could not be brought closer together than about 4 microns when the surfaces were submerged in water. However, Bastow and Bowden (1932) found that elaborate techniques were necessary to exclude dust and other solid particles from surfaces. When this was done, surfaces polished to 0.25 microns were easily brought together until their asperities essentially touched, whether they were in air, vacuum, or water.

Bastow and Bowden (1935) also measured the viscosity of thin liquid films between flat surfaces of metal and glass. Measurements were made down to 0.1 micron, where the surface asperities touched. No change in the viscosity of water was measured, even at a separation of 1000 \AA .

The thickness of an adsorbed layer can be calculated from adsorption experiments. If the amount of adsorbate is determined by weight changes, however, the calculated thickness may not represent the actual surface conditions.

Bowden and Throssell (1951), using two separate techniques, found that the calculated thickness of water adsorbed on metal surfaces depended on the method of preparing the surface and the technique used to measure the adsorption. If the surface was not strongly heated, the apparent adsorption (by measuring weight changes on a micro-balance) was a layer 20 molecules thick at 95% of the saturation pressure. If, however, the surfaces were cleaned by heating to a red heat, and then water vapor adsorbed on them, the layer was only two molecules thick at the same relative pressure. If a clean surface was washed with tap water, the weight changes again indicated a thick adsorbed layer.

Independent measurements were made using the ellipticity induced in plane polarized light reflected from the surface as a

measure of the thickness of the adsorbed layer. By this technique it was shown that even at 95% of the saturation vapor pressure the film thickness was less than two molecules thick, for both the heat treated and the normal surfaces.

The high apparent adsorption obtained by weight changes was attributed to hygroscopic contaminants such as KOH. The contaminant would tend to take up water until the resulting KOH solution had a vapor pressure equal to the vapor pressure in the system. At a relative pressure of 0.5, 10^{-7} gm/cm² of KOH would give rise to an "adsorption" of 1.5×10^{-7} gm/cm² of water--equivalent to 5 molecular layers. At a relative pressure of 0.9 the apparent adsorption would be 25 layers.

In the light reflection experiments the adsorption was the same for both clean and contaminated surfaces. The inference is that the adsorbate collects around the regions of contamination. In the optical method this merely increases the scattered light (which is not measured) while the reflected light (which is measured) represents the adsorbed thickness on the rest of the surface.

Derjaguin and Zorin (1957) found that multimolecular adsorption occurred on glass at relative pressures above 0.95. At $p/p_c = 0.98$, they measured about 10 molecular layers. The water tension at this pressure can be calculated by the following equation (Schofield, 1935):

$$\ln \frac{p}{p_0} = - \frac{Mhg}{RT} \quad (4.6)$$

where p/p_0 = relative pressure
 M = molecular weight of water
 h = head in cm water
 g = 981 cm/sec²
 R = 8.3×10^7 ergs/mole °K
 T = absolute temperature °K

At $p/p_0 = 0.98$, h is 3×10^4 cm. or about 425 psi. To maintain a 30 Å thick water layer under this tension would require larger forces than can be explained by the equations generally used to compute van der Waals and double layer attractions.

Although some ambiguity exists regarding the thickness of the adsorbed layers at pressures approaching saturation, there is no doubt that under high vacuum conditions the amount of physically adsorbed gas will be a small fraction of a monolayer, even at room temperature. A chemisorbed layer may exist at very low pressures, and the conditions required to remove such a layer are discussed later in this chapter.

Mobility of the Adsorbed Layer

A great deal of controversy exists regarding the mobility of gases adsorbed on a solid. Again, this is largely due to the lack of incontrovertible data.

Direct mobility measurements indicate that the activation energy for surface diffusion is about 30% to 60% of the adsorption energy for chemisorbed ions (Ehrlich, 1959; Brunauer, 1945, p. 452), and that appreciable surface migration occurs at one quarter to one half of the absolute temperature required for appreciable evaporation.

Direct evidence of surface mobility for physically adsorbed atoms is lacking. A molecule should be able to move along the surface if its average thermal energy in the two degrees of freedom parallel to the surface (kT) exceeds the energy barrier due to the surface bonding forces. At room temperature the molecular thermal energy is only 0.6 Kcal/mole, so the barrier must be quite small for the adsorbed molecules to have mobility.

The calculated height of the energy barrier for argon on KCl is only 0.08 Kcal/mole, or about 5% of the adsorption energy (Gregg, 1961, p. 20). Actual measurements of the mobility have not been

made, however. It is quite likely that the energy barrier to migration of physically adsorbed molecules is a small percentage of their adsorption energy, and in many cases may be less than 0.6 Kcal/mole. In which case, these molecules would have surface mobility.

Measurements of the differential entropy of adsorbed molecules are often used to draw conclusions regarding their movement and arrangement on the surface. This requires a comparison of experimentally determined values with those calculated from a reasonable molecular model. Various restraints are applied to the molecules in the model until the calculated entropy values agree with the measured values. The number of restraints which can be applied are so numerous (up to 9 for a non-linear triatomic molecule) that unambiguous interpretation is often impossible. For example, it is generally very difficult to distinguish between a localized molecule with free vibration and rotation and a mobile molecule (two-dimensional fluid) with limited rotation.

Even though physically adsorbed molecules may be sufficiently mobile to exchange places with each other, they may be very difficult to remove completely from adsorption sites. Fig. IV-2 shows two idealized surfaces under pressure p , each with a monolayer of adsorbate. To conserve energy, the work done in bringing the two surfaces closer together must be equal to the change in energy of the adsorbate in going from an adsorbed site (M_a) to the atmosphere (M_b). All sites are assumed equivalent with a desorption energy Q . The pressure required is given by

$$p \Delta V = Q \quad (4.7)$$

The volume change per unit area is d , the diameter of the adsorbed gas. Therefore,

$$p \approx \frac{1.45 \times 10^3 Q}{d} \quad (4.8)$$

p = pressure in p.s.i.

Q = desorption energy in ergs/cm²

d = diameter of molecule in angstroms

van Olphen (1963), using adsorption isotherm data, evaluated the work of desorption of the last layer of water from calcium montmorillonite as 140 ergs/cm². Putting this into equation 4.8 gives 68,000 psi as the pressure required to remove the adsorbed water.

D. Desorption of Surfaces Under High Vacuum

Desorption of a solid surface involves two steps:

- 1) Removing the initially adsorbed material
- 2) Preventing readsorption from the gas phase

Both of these processes should be amenable to theoretical analysis. Removing the initially adsorbed material involves the use of pressures and temperatures such that the equilibrium constant for desorption, K_p , is large. K_p is determined from the following equation:

$$-\Delta F = RT \ln K_p \quad (4.9)$$

where ΔF is the free energy change for the desorption process.

Due to incomplete knowledge regarding the nature of the bonding which occurs for most adsorption processes, it is not generally possible to write a chemical equation which will permit accurate calculation of reaction constants. The conditions required to prevent readsorption on a clean surface can be approximately determined, however, and this knowledge can be used as a guide for predicting desorption conditions.

A simple experiment for determining the adsorption energy for a solid-gas system would be to heat the solid to a temperature T , at a pressure p , such that all of the adsorbed gases were driven off the surface. The temperature is then lowered to T_2 , at which point readsorption occurs. Appendix II presents an analysis of this situation and gives a method of calculating either the adsorption energy, temperature, or pressure if the other two variables are known.

The results of the analysis indicate that a gas molecule which adsorbs on a solid surface at a temperature T ($^{\circ}\text{K}$) and a pressure p (mm Hg) must have a minimum adsorption energy Q (cal/mole) given by

$$Q = T \ln T + 4.6 T (6 - \log_{10} p) \quad (4.10)$$

The first term of the equation generally represents less than 10% of the total, so between 200 and 2000 $^{\circ}\text{K}$, equation 4.10 may be written as

$$Q = 5.1T (6 - \log_{10} p) \quad (4.11)$$

giving a linear plot of Q vs. T for a given pressure. Values of Q and T for various vacuum levels are plotted in Fig. IV-3.

Figure IV-3 can be used to determine the approximate conditions required to prepare and maintain a clean surface. For example, molecules with adsorption energies larger than about 25 Kcal/mole cannot be removed even at very low pressures without using elevated temperatures. On the other hand, molecules with adsorption energies less than 15 Kcal/mole will not adsorb on a surface at pressures of 10^{-4} torr, even at room temperature. It should be noted that Fig. IV-3 is for equilibrium conditions, and says nothing about the time required to reach equilibrium. As a practical matter temperatures somewhat larger than those indicated on the graph should be used to desorb surfaces.

If the surface to be cleaned is known to have a gas with an adsorption energy Q on it, various combinations of temperatures and pressures may be used to clean the surface. For example, gas with $Q = 50$ Kcal/mole may be removed by the following combinations of pressure and temperature:

$$\underline{Q = 50 \text{ Kcal/mole}}$$

<u>p (torr)</u>	<u>T (°C)</u>
10^{-12}	260
10^{-10}	330
10^{-8}	420
10^{-4}	700

Since temperatures somewhat larger than those indicated should actually be used to achieve desorption in a reasonable period of time, the advantage of using low pressures is readily seen. In addition, once the surface is cleaned, it may be desirable to reduce the temperature to run the experiment. Then low pressures must be used to prevent appreciable readsorption during the time required to run the experiment, as explained in Chapter II.

Figure IV-3 indicates that very high temperatures may be required to remove chemisorbed gases with high adsorption energies. At these temperatures other surface phenomena, such as sintering and surface rearrangements, may occur thus altering the surface. This may have important consequences for mineral surfaces.

Surface Mobility and Surface Rearrangements

The surface atoms of a solid are normally immobile. At a temperature above 0.3 of the melting point, T_m (°K), some surface migration can occur. Near 0.5 T_m the rate of migration and diffusion rapidly increases, and sintering begins to occur (Gregg, 1961). Clearly, a material which must be heated above this temperature to desorb the surface may not have the same surface arrangement of atoms or surface energy as it would have at a lower temperature. For metals, surface rearrangements may be of little consequence, but for minerals with covalent bonding the surface may be drastically altered, as a consideration of the dehydration of silica surfaces will show.

The Surface of Desorbed Silica

A quartz crystal which is broken in an ultra-high vacuum will have two charged surfaces which, due to the lack of adsorbate molecules and the immobility of the atoms in the solid, may retain its initial structure for a considerable time. If the broken surfaces are put back into contact, they may strongly readhere.

Attempts to reproduce this situation by placing two quartz blocks in an ultra-high vacuum and desorbing the surfaces may be unsuccessful. The hydrated silanol surface, when heated, may decompose to form a siloxane surface, as shown in Fig. IV-4. The siloxane surface is not charged, and has a low surface energy, less than 200 ergs/cm^2 . If two such surfaces are brought into contact, the adhesion will be very small, probably even less than between clean silanol surfaces. This could be checked experimentally by measuring values of the coefficient of friction in a vacuum at temperatures below that required to decompose the silanol surface, and at higher temperatures where a siloxane surface is formed.

Experiments on glass indicate that dehydration of the OH surface groups can be reversible if the temperature is not above 400°C . (Holland, 1964, p.288). Silica glass heated above 400°C could not be rehydrated except by soaking in liquid water, indicating that a siloxane surface had formed.

Langmuir* noted that at temperatures less than 500°C , water desorption from glass under 10^{-3} torr vacuum would cease after about $\frac{1}{2}$ hour of heating. Raising the temperature would then result in additional gas evolution, which would again stop within one half hour. Complete removal of surface OH groups and adsorbed H_2O could be obtained at 400°C , without forming a siloxane surface. At temperatures above 600°C , water evolution continues indefinitely, as shown in Figure IV-5, due to migration of OH^- ions from the interior

* These experiments are described by Holland (1964, p. 214).

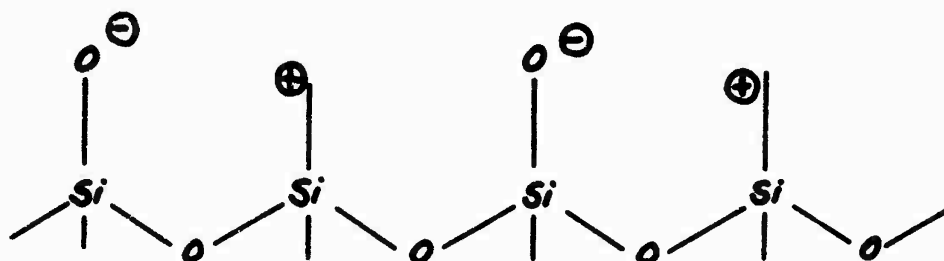
(Holland, 1964, p.214). The concentration of OH^- ions in glass is extremely high for high vacuum purposes, and greatly complicates the interpretation of surface studies on glass. The lowest hydroxyl content is found in fused silica, which has about 3×10^{-4} wgt. per cent OH^- ions, or about 10^{18} - 10^{19} OH^- ions/cm³ of glass (Holland 1964, p. 249).

All of the processes by which water is bound to silica, and the rearrangements of surface structure which occur due to heating and desorption are not known. It may be possible to desorb quartz or glass in a vacuum and produce a very active clean surface. But dehydration of the surface may be accompanied by surface rearrangement and siloxane formation, leading to a low energy surface.

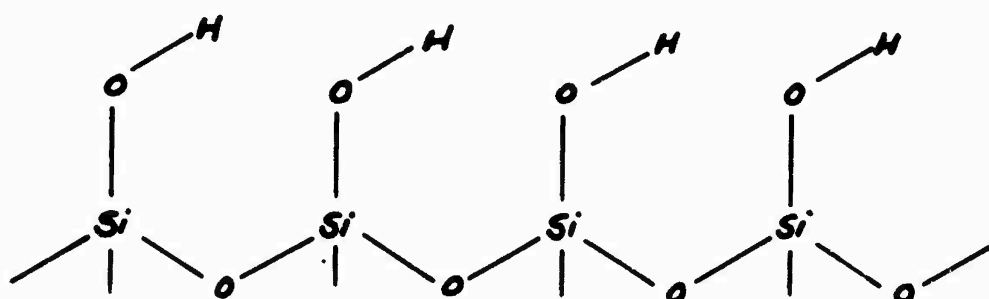
Table IV-I Adsorption Times for Various Adsorption Energies

<u>Q</u> <u>Kcal/mole</u>	<u>T</u> <u>°K</u>	<u>τ</u> <u>sec.</u>	<u>Remarks</u>
1.0	300	5×10^{-13}	essentially no adsorption
5.0	300	4×10^{-10}	
10	300	2×10^{-6}	limit of physical adsorption
20	300	50	chemisorption
20	600	2×10^{-6}	increasing temp. reduces residence time to physical adsorption range
30	300	1×10^9	(300 years)
100	300	10^{150}	

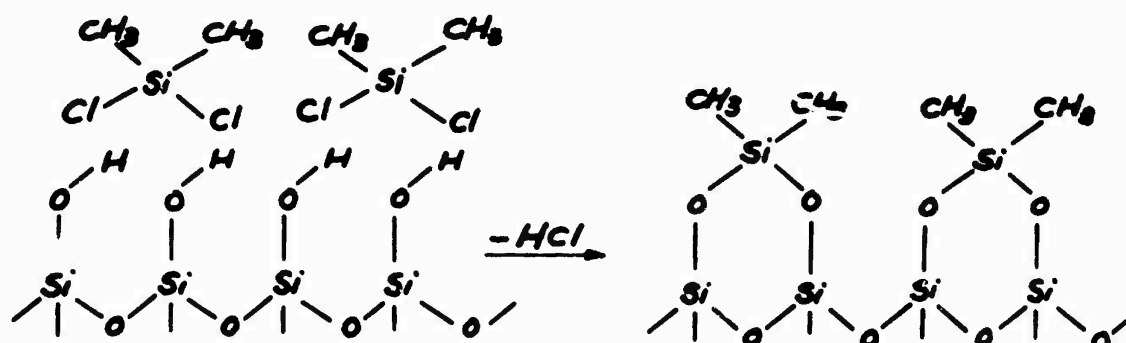
The Surface of Quartz



a) Freshly broken quartz surface



b) Hydrated quartz silanol surface



c) Hydrophobic quartz surface

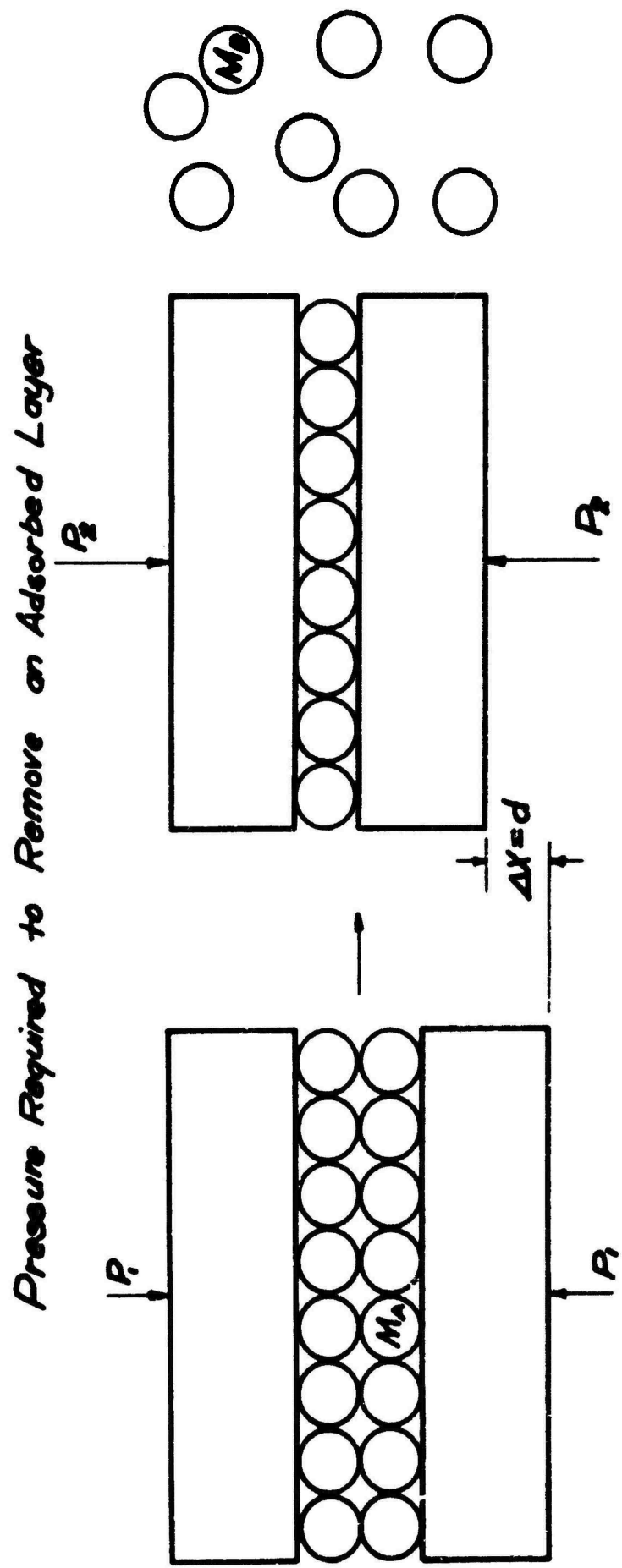


Figure II-2

Temperature and Pressure Conditions for Desorption

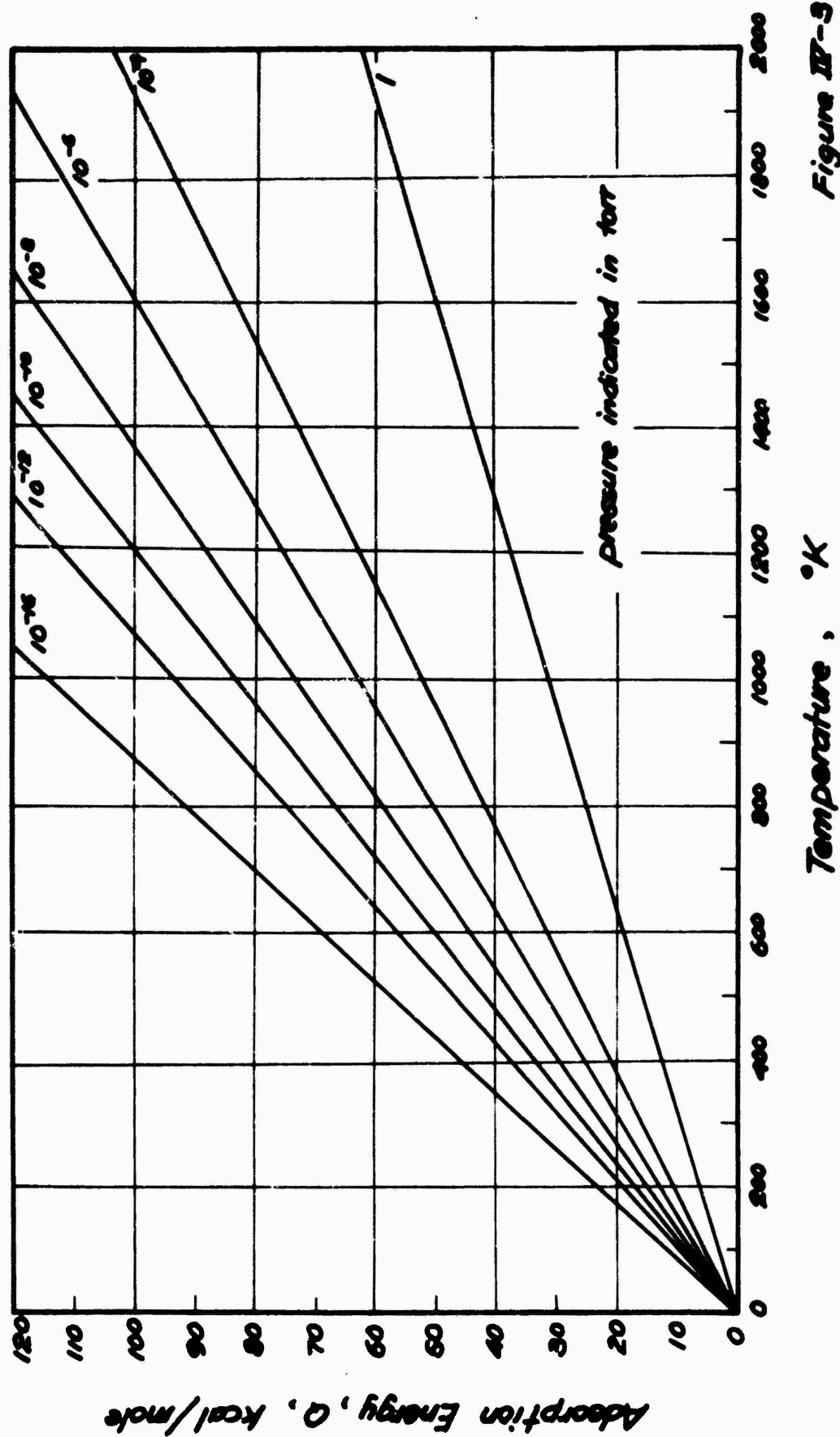


Figure II-3

Desorption of a Quartz Surface

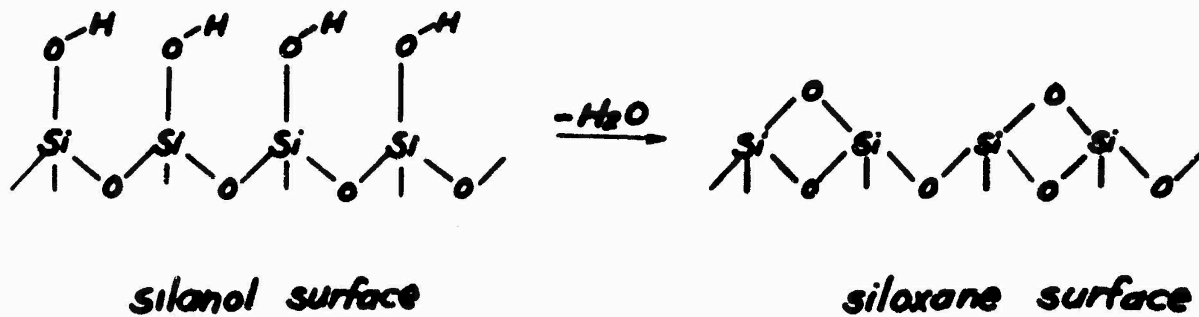


Figure IV-4

Evolution of Water from Glass

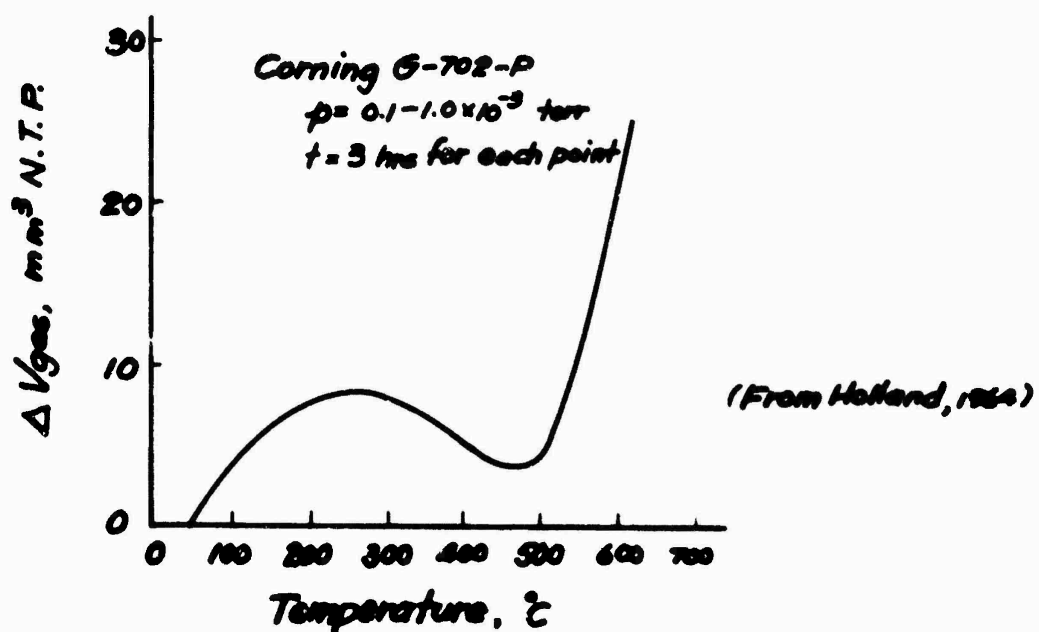


Figure IV-5

V. FRICTION AND COHESION OF SOLID SURFACES

The two basic laws of friction, originally postulated around 1500 by Leonardo da Vinci and revived by Amontons in 1699, are as follows:

- 1) The frictional force is directly proportional to the normal force applied to the surfaces.
- 2) The frictional force is independent of the total area of the surfaces.

Initial attempts to explain these laws employed the interlocking of projections on the uneven surfaces. The coefficient of friction, μ , would then be given by the tangent of the average angle of the surface irregularities. Sir W. Hardy (1936) pointed out that this explanation would require a lower μ as the surfaces became smoother, becoming zero for a perfectly smooth surface. In actual fact, μ is found to be constant over a wide range of surface roughness. Hardy concluded that static friction is due to cohesive forces between the contacting surfaces, and verified this by microscopic examination of the wear track produced by sliding glass surfaces over one another. Hardy also realized that the actual area of contact was only a small fraction of the total area, and that the cohesive forces on a unit area basis were therefore quite large.

In 1925 Terzaghi provided a physical explanation and a mathematical description of the friction process (Skempton, 1960). Terzaghi reasoned that the normal load, W , acting on the very small area of actual contact would cause yielding of the contacting asperities. The contact area, A_c , would thus be given by

$$W = A_c \sigma_y \quad (5.1)$$

where σ_y is the yield stress of the material. If the material is assumed to have a constant shear strength τ_m , then the maximum tangential force F , which can be applied is

$$F = A_c \tau_m \quad (5.2)$$

The coefficient of friction is then determined by

$$\mu = \frac{F}{W} = \frac{\tau_m}{\sigma_y} \quad (5.3)$$

Terzaghi's analysis was later proposed independently by Bowden and Tabor (1950) and shown by them to explain the frictional behavior of a wide variety of materials. The Terzaghi-Bowden-Tabor analysis, commonly called the Adhesion Theory of Friction, is now the basis for all frictional studies.

A. The Adhesion Theory of Friction

The area of contact will generally be determined by the mechanical properties of the solid and will be related to the stress required to deform the material, as indicated by equation 5.1. The amount of actual solid to solid contact, and hence the shear strength of the contact, will be largely determined by the type and amount of material adsorbed on the surface.

The friction measured under atmospheric conditions is seldom, if ever, between clean surfaces as they are defined in this report. Normally, actual solid contact occurs over a fraction δ , of the contact area. Over the rest of the area, $(1-\delta) A_c$, the contaminant film is not broken and the shear strength, τ_2 , is lower than that of the solid, τ_m . The total frictional force, F , will be

$$F = A_c [\delta \tau_m + (1-\delta) \tau_2] \quad (5.4)$$

Actual values of δ and τ_2 cannot generally be measured, and equation 5.4 has little practical value.

As the surfaces become cleaner, it is found that the adsorbed layer not only affects the strength of the junctions, but also the area of contact. If the material behaves plastically, it will deform under combined compressive stresses (σ) and shear stresses (τ) according to the von Mises-Hencky criterion (Nadai, 1950, p.248), which in two

dimensions is given by

$$\sigma^2 + 3\tau^2 = \sigma_y^2 \quad (5.5)$$

where σ_y is the uniaxial compressive strength. If the asperities are initially loaded to $\sigma = \sigma_y$, then application of a small τ will require that σ become less than σ_y . This can only happen if the contact area increases. As τ increases the contact area must continue to increase to maintain plastic equilibrium. If the junction does not shear until $\tau = \tau_m$, the shear strength of the bulk solid, then σ_y must decrease to zero, which requires an infinite area of contact, or gross seizure over the entire area.

The conditions for sliding when the shear strength of the junctions is less than that of the bulk solid have been calculated by Bowden and Tabor (1964, p. 75). If τ_i is the shear strength of the junctions and τ_m is the shear strength of the bulk solid, then

$$\sigma^2 + \alpha \tau_i^2 = \beta \tau_m^2 \quad (5.6)$$

For the three dimensional state of stress acting at the contact points, α and β are not rigorously known. However, Bowden and Tabor show that they can be expected to have a value between 9 and 25.*

By assuming that $\alpha = \beta$, equation 5.6 can be rewritten as follows:

$$\sigma^2 = \beta \tau_i^2 \left(\frac{1 - k^2}{k^2} \right) \quad (5.7)$$

where $k = \tau_i / \tau_m$

* This is essentially a bearing capacity analysis, where σ is the unit applied stress. The ratio of $\frac{\sigma}{\tau_m}$ will vary between 3 and slightly more than 5 depending on the geometry of the contact. Fortunately, the actual value of this ratio has little effect on the results of the analysis, as will be shown.

Therefore,

$$\mu = \frac{F}{W} = \frac{\tau_i A_c}{\sigma A_c} = \frac{1}{\sqrt{\beta} \left(\frac{1 - k^2}{k^2} \right)^{1/2}} \quad (5.8)$$

Figure V-1 (from Bowden and Tabor, 1964, p. 76) is a plot of μ vs. k for various assumed values of β . It is seen that the value of β has relatively little effect on shape or position of the curves. The friction is infinite for $k = 1$, but for k only slightly less than one the friction has dropped to a reasonable value.

If the axial pressure required to cause plastic yielding is taken as σ_o , where $\sigma_o = \frac{W}{A_{co}}$ for $F = 0$, equation 5.6 may be rewritten as

$$\sigma^2 + \alpha \tau_i^2 = \sigma_o^2 \quad (5.9)$$

Realizing that $\sigma = \frac{W}{A_c}$, when F is greater than zero, equation 5.9 leads to the following relationship between the increase in contact area $\left(\frac{A_c}{A_{co}} \right)$ and the ratio $\frac{F}{W}$:

$$1 + \alpha \left(\frac{F}{W} \right)^2 = \left(\frac{A_c}{A_{co}} \right)^2 \quad (5.10)$$

Figure V-2, from Bowden and Tabor (1964, p. 76) is a plot of equation 5.10 for $\alpha = 9$ (again the actual value is not critical). For clean surfaces, $k = 1$ and $\frac{A_c}{A_{co}}$ increases indefinitely (gross seizure). Limiting values of $\frac{A_c}{A_{co}}$ and $\frac{F}{W}^*$, at which slip would occur, are indicated for other values of k . For $k = 0.99$, the contact area increases about 7 fold before the junction shears. For $k < 0.9$, the area increase is very small.

* The limiting value of $\frac{F}{W}$ is μ , the coefficient of friction.

Qualitative verification of the preceding analysis has been obtained for many metals which are capable of extensive plastic deformation. Bowden and Young (1951) degassed two iron surfaces at 1000°C and 10^{-6} torr, cooled them to room temperature, and measured $\mu = 3.5$. However, when the surfaces were reheated to 300°C and placed together under a normal load of 14 grams, seizure occurred, the friction was higher than the maximum tangential force which the system could apply, and no visible sliding occurred. When the specimens were removed from the vacuum, a tensile force of 1.18 Kg was required to break them apart. From photomicrographs the real area of the welded junctions was found to be 0.0187 mm.^2 , giving a strength of 90,000 psi. The measured contact area had increased by more than a factor of 100 over its calculated value under the normal load only.

The validity of the adhesion theory of friction and the concepts of junction growth for clean surfaces have been conclusively demonstrated for plastic materials.

B. Theory of Friction for Elastic Solids

The contact area of a perfectly elastic material will not be given by a plastic yield equation. If the asperities are assumed to have spherical tips, the classical Hertz analysis may be applied, which predicts a plane circular contact of diameter d given by:

$$d = (\delta WR)^{1/3} \quad (5.11)$$

where W is the normal load, R is the radius of the tip, and δ is determined by the contact conditions and the elastic constants of the material (Timoshenko and Goodier, 1951, p. 372). For a spherical indenter on a plane surface δ is given by

$$\delta = \frac{12 (1 - \nu^2)}{E} \quad (5.12)$$

The contact area will thus be given by

$$A_c = K W^{2/3} \quad (5.13)$$

where $K = \frac{\pi}{4} (\delta R)^{2/3}$

The frictional force and μ will be

$$F = \tau_i A_c = \tau_i K W^{2/3} \quad (5.14)$$

$$\mu = \frac{F}{W} = \tau_i K W^{-\frac{1}{3}} \quad (5.15)$$

The coefficient of friction will vary as the minus one third power of the normal load, but the adhesion theory should still be valid for explaining the frictional behavior.

The preceding analysis, which is for a single asperity on a flat plane, may not accurately describe the complex contact conditions between two surfaces which have a very large number of asperities. In this situation elastic deformation can occur by two mechanisms (Archard, 1957):

- 1) As the load increases the number of contacting asperities remains constant and the elastic deformation of each asperity increases. In this case the contact area is proportional to $W^{\frac{2}{3}}$.
- 2) As the load increases the number of contacting asperities increases proportionally and the deformation of each asperity remains essentially constant. The area of contact is proportional to W .

In an actual situation, the area of contact may be expected to vary as W^n , where n is between $\frac{2}{3}$ and 1. By choosing a model where the main asperities have still smaller asperities on their surfaces, Archard calculates $n = \frac{44}{45}$, thus demonstrating that even elastic materials may follow Amonton's Law and have an approximately constant μ .

Experimentally, it may be difficult to vary W over a sufficiently wide range to accurately measure the variation of friction with load. Rowe (1962) varied the normal load on quartz by a factor of 50 and found a maximum variation of only 1° in $\tan^{-1} \mu$, which is within the experimental error. By varying the particle size in his shearing apparatus, however, he was able to vary the load per particle by a factor of almost 10,000. The results of his tests are plotted in Fig. V-3. The angle of friction ($\phi_\mu = \tan^{-1} \mu$) decreases as the particle size (and load per particle) increases. In Figure V-4, Rowe's data are replotted as $\log \mu$ vs. the load per particle, also on a log scale. Except for the point at the highest load, the data falls on a straight line with a slope of -0.05. This indicates a value of n of $\frac{19}{20}$. The possibility of some load-bearing particles rolling, rather than sliding, on the shear plane may have influenced these results. Also, variations in particle roughness may have had some effect. Further tests are needed to verify Archard's analysis and to determine the variation of μ with load for quartz and other minerals.

The Frictional Behavior of Diamond

Although diamond may be made to deform plastically at high temperatures, permanent indentation at room temperature is not generally observed. Bowden and Tabor (1964, p. 162) used loads on a spherical indenter corresponding to 2000 kg/mm^2 (2,800,000 psi), where cracking occurred at the edges of the circle of contact. The tensile stress in the region of cracking was calculated as 400 kg/mm^2 , which corresponds to the tensile strength of diamond as measured in bending tests. Permanent plastic deformation was not observed, even at these high loads.

It is found that as the radius of the indenter decreases the stress required to cause cracking increases. This may be because the smaller indenter tip only affects the small Griffith cracks and not the larger ones. Thus by using extremely small indenters (around

1 micron) it may be possible to cause plastic deformation in diamond before cracking occurs. An indication of this has been obtained by studying reflection electron micrographs of the wear tracks on diamond surfaces (Bowden and Tabor, 1964, p.166). Small tracks outside of the main track, apparently caused by very small asperities, have rounded edges and the "smeared" appearance of plastic flow.

Plastic Deformation of Quartz

Quartz can deform both elastically and plastically at room temperature, and its frictional behavior may be expected to bear similarities to both metals and to diamond. On a relative scale, quartz is fifty times harder to deform plastically than rock salt, and diamond is ten times harder than quartz.

Hardness is expressed as the normal force applied to an indenter in contact with a solid surface divided by the measured area of deformation after the indenter is removed. The punching action of a hardness indenter causes a bearing capacity failure in the indented solid. The indentation hardness of a material is thus a measure of its resistance to plastic deformation. For quartz and other brittle materials, a pyramidal indenter of diamond, such as the Vickers or the Knoop indenter, is used to minimize cracking (Brace, 1960). It is found that a normal pressure of 1100 kg/mm^2 or 1,500,000 psi is typically required to produce plastic deformation in quartz. The maximum size of indentation is around 100 microns. For lengths greater than this, wholesale fracturing occurs (Brace 1963). A reason for the cracking caused by larger indentations was given above in the discussion of plastic flow in diamond.

The apparent ductility of normally brittle materials such as quartz is due to the high confining pressures developed in the contact region. The stress-strain field under the tip of an indenter has not been completely analyzed. However, Brace (1960 and 1963) estimated

the compressive strength, $(\sigma_1 - \sigma_3)_{\max}$, to be $1/3$ of the hardness, which gives $(\sigma_1 - \sigma_3)_{\max} = 500,000$ psi at a confining pressure $\sigma_3 = 290,000$ psi for quartz. These values may be low, as will subsequently be shown.

It is interesting to note that Bridgman (1952), in his studies of plastic flow under high confining pressures, was never able to cause plastic deformation in quartz. He measured $(\sigma_1 - \sigma_3)_{\max} = 570,000$ psi at a confining pressure of 360,000 psi with no detectable plastic deformation. This indicates that the value of σ_3 required to prevent brittle fracture in quartz is higher than predicted by applying plasticity theory to hardness measurements. However, non-uniform stress conditions in the triaxial device which Bridgman used may have induced a brittle failure. In particular, stress concentrations and restraints at the end platens could have started a crack which propagated before appreciable plastic flow occurred.

The results of Bridgman's tests on quartz are plotted in Fig. V-5 using Mohr's circles. The envelope to the circles gives $c = 130,000$ psi and $\phi = 14.5^\circ$.

Bridgman's results can be combined with an analysis of the hardness test given by Bowden and Tabor (1964, p. 335) to shed more light on the deformation of quartz. Bowden and Tabor state that the ratio of hardness (H) to strength $(\sigma_1 - \sigma_3)$ is a function of the ratio $E/(\sigma_1 - \sigma_3)_u$, where E is Young's modulus and $(\sigma_1 - \sigma_3)_u$ is the unconfined strength (σ_y for a plastic material). For $E/(\sigma_1 - \sigma_3)_u > 200$, the ratio $H/(\sigma_1 - \sigma_3)$ is approximately equal to 3. This is the situation with most metals. However, for $E/(\sigma_1 - \sigma_3)_u < 200$, $H/(\sigma_1 - \sigma_3)$ is less than 3 and should decrease as $E/(\sigma_1 - \sigma_3)_u$ decreases.*

* The analogy with a bearing capacity problem occurs here also. The geometry of the indenter results in a "bearing capacity factor" of 3 for a plastic material. For a material with a low ratio of $E/(\sigma_1 - \sigma_3)_u$, larger strains can occur within the elastic limit. Therefore, the material under the indenter is less restrained than it would be if it were a rigid plastic solid, and a lower bearing capacity results.

For glass, Bowden and Tabor give $H / (\sigma_1 - \sigma_3) = 1.5$.

For quartz, calculations indicate that $E / (\sigma_1 - \sigma_3)_u$ is only about 44^{*}. Since this value is so much less than 200, $H / (\sigma_1 - \sigma_3)$ should be very low, perhaps less than the value for glass. Fig. V-5 can be used to calculate a minimum value of $H / (\sigma_1 - \sigma_3)$ by taking $\sigma_1 = H$, thus maximizing $(\sigma_1 - \sigma_3)$. The dashed circle in Fig. V-5 shows this condition and indicates a value of $(\sigma_1 - \sigma_3) = 800,000$ psi. Therefore, the minimum possible value of $H / (\sigma_1 - \sigma_3)$ for quartz is $1,500,000/800,000$ or 1.9.

There is no easy mechanism whereby quartz can deform plastically. The strong three dimensional framework of silica tetrahedra prevents any easy slip system, which is why quartz does not show easy cleavage. Quartz twins readily, but the only twinning mode which has been shown to result from mechanical forces, the so-called Dauphine mode parallel to the vertical axis ($10\bar{1}0$), does not result in external deformation of the crystal. Westbrook (1958) concluded that the apparent plastic flow that occurs during deformation of quartz cannot be understood in terms of known deformation mechanism. Recent data (Brace, 1963) indicates that the permanent deformation may be a result of micro-fracturing on a scale too small to be observed.

It is clear that very high stresses are necessary to cause plastic flow in quartz. Brittle failure will generally occur before a quartz soil particle reaches a sufficiently high stress to deform plastically. If plastic deformation occurs it will be restricted to

* E for quartz varies with crystallographic orientation (Brace and Walsh, 1962). A value of 15×10^6 psi, which is close to an upper limit, was chosen for this calculation. The value of $(\sigma_1 - \sigma_3)_u$ was determined from Figure V-5 as 340,000 psi, using the Mohr circle with $\sigma_3 = 0$.

small asperities which are highly confined.

The Frictional Behavior of Quartz

Is the friction of quartz determined by elastic deformation, as for diamond, or by plastic flow, as for metals? This is a difficult question to answer, for the behavior will vary with the size and roughness of the loaded area, and the magnitude of the load.

For example two quartz blocks, each with a surface area of 1 cm^2 , may be imagined to contact at only three asperities. If they are reasonably smooth surfaces, the effective radius of the asperities may be about 1000 \AA . To cause these 3 contacts to deform plastically would require a load of only a fraction of a gram. If, however, the surfaces are assumed to be covered with uniform asperities of this size, such that about $1/2$ of the planar surface area has asperities, then the deformation will be elastic up to a load of about 10,000 lbs.

In a granular soil, the particles are generally rough, and the surface asperities would be at least of the size used above. For the smaller sized (silt) particles, with a particle diameter of only $20,000 \text{ \AA}$, the area of contact with another particle would also be small, possibly involving only one asperity of 1000 \AA radius or less. However, if all of the particles are this small, the average load per particle will be only about 3×10^{-4} gram at a confining pressure of 100 psi.

A hemi-spherical quartz asperity of 1000 \AA radius would require a load of 6×10^{-4} gram for plastic flow. Thus, while it is possible to envision very small quartz particles under high loads deforming plastically at the contacts, under most conditions deformation of an "average" quartz surface may be expected to proceed as follows:

- 1) When the surfaces are first brought into contact under very light loading, the highest surface asperities will carry the load. If they are few in number, these highest points may deform plastically.

- 2) As the loading is increased, more asperities will be brought into play and although the initially highest points may be deforming plastically, most of the load will probably still be carried by elastic deformation.
- 3) If the surface only makes one contact with each of two adjacent surfaces (the minimum equilibrium conditions), as, for example, might occur with a silt-sized particle, the deformation will depend on the load carried by the particle. At high loads, if the load continues to be carried through a single asperity, this asperity will be plastic.

C. Friction and Cohesion of Clean Surfaces

The existence of surface forces should bring about cohesion of two solid surfaces whenever such surfaces are brought within atomic range. Two reasons why large scale cohesion or "cold-welding" is seldom observed have been given:

- 1) Adsorbed gases reduce the net surface attraction.
- 2) Real surfaces are, with few exceptions, very rough on a molecular scale, and the solids actually contact over a very small area.

If the adsorbed gases are removed by heating in a high vacuum and if the solid behaves plastically, large scale seizure is observed, and large cohesive forces develop.

The effect of adsorbed gases on the friction and cohesion between surfaces has been studied by using freshly cleaved mica surfaces, which eliminates complications due to surface roughness.

Cohesion Between Mica Surfaces

The measured surface energy of mica cleaved in air is about 300 ergs/cm^2 (Bailey and Courtney-Pratt, 1955). Cleavage in an ultra-high vacuum of 1×10^{-13} torr requires $5,125 \text{ ergs/cm}^2$, indicating

that the low value in air is due to rapid contamination of the surfaces (Bryant, 1962). Repeated opening and closing of the mica sheets in the vacuum showed little loss of the high surface energy. If helium, argon, or nitrogen gas was admitted to the vacuum, the cohesion remained at a high level. If oxygen or water vapor were admitted, however, rapid adsorption occurred and the surface energy dropped to the in-air value.

The high surface energy of mica is due to the charged surface which results when the sheet is cleaved (mica sheets are held together by potassium ions). The energy required to cleave talc or pyrophyllite, which are held together by weak van der Waals bonds, does not show a large increase in vacuum.

Bailey and Courtney-Pratt (1955) measured the friction and cohesion between molecularly smooth surfaces of mica. Thin sheets of mica were bent into cylindrical shape, and the contact was between two crossed cylinders. By using optical interferometry, they were able to measure the area of contact and the separation between the sheets very accurately.

When the sheets were first put into contact, an interfacial film of $6 \pm 2 \text{ \AA}$ thickness was measured, indicating monolayer adsorption (probably water) on each surface. Separation of the sheets required a tensile force, which when divided by the measured contact area at separation, gave an adhesion stress of 2 Kg/mm^2 or 2800 psi (independent of the initial normal load W), indicating a large amount of cohesion despite the adsorbed layer.

The friction was found to vary with load as shown in Fig. V-6. Due to the attractive forces between the sheets a finite area of contact could be obtained with no external loading, leading to an infinite coefficient of friction. As the loading increased, the contribution of the external load to the total contact area increased, and μ dropped to a value of 35. However, the friction force always was found to be

proportional to the contact area at the onset of sliding, as shown in Figure V-7. The slope gives an interfacial shear strength of 10 Kg/mm^2 or 14,000 psi, reproducible within $\pm 10\%$.

Sliding was accompanied by a large amount of surface damage, indicating that shear was not confined completely to the adsorbed layer. When an organic monolayer (calcium stearate) was added, the shear strength dropped to 355 psi, and no damage to the surface occurred at slow rates of sliding.

The reason for the extensive surface damage is not known. By using a reflection electron microscope, Bailey and Courtney-Pratt determined that no small-scale isolated irregularities greater than 30 \AA existed. Therefore, they concluded that no appreciable solid-solid contact through the adsorbed film occurred. This leads to a considerable shear strength for the adsorbed film. Although the data seem to support this conclusion, particularly in the case of the damage-free calcium stearate coated surfaces, conclusive proof has not been given that no solid-solid contact occurred through the adsorbed layers.

Cohesion of Elastic Solids

The friction of diamond under atmospheric conditions is very low ($\mu \sim 0.05$) and the shear strength of the junctions is a small fraction of the bulk shear strength of diamond (Bowden and Tabor, 1964, p. 170). If the surfaces are cleaned by heating in a high vacuum, μ increases to about 0.5 and the shear strength of the interface is found to be approximately equal to that of the bulk solid (1200 Kg/mm^2).

Because diamond behaves elastically, junction growth by plastic flow and consequent gross seizure do not occur. Furthermore, no cohesion is measured. That is, if the normal load, W , is reduced to zero, the surfaces separate. Because the material has not deformed plastically, any junctions which formed under the compressive load are broken by elastic rebound when the load is removed (Bowden and Tabor, 1957).

King and Tabor (1954) measured the friction and cohesion of clean rock salt, which has a Vicker's hardness H_v , of 17 Kg/mm^2 . The highest value of μ obtained was 1.3. No junction growth has been observed for rock salt, glass, or sapphire.

It does not seem likely that quartz or other minerals would exhibit large scale seizure or "cold-welding", even at high temperatures in a high vacuum. The coefficient of friction should increase appreciably due to the increased strength of the junctions, but the possibility of a mass of quartz particles aggregating to form a rock-like material seems remote.

Large-scale seizure, even of clean surfaces, can only occur if the contact area is large. With ductile materials, the contact area becomes large as a result of plastic junction growth. However, quartz does not deform plastically under shear stresses only. It must have a large confining pressure. Even if a quartz asperity were heavily loaded and plastically deformed, a drop in confining pressure upon application of a shearing stress would prevent further plastic flow.

It is doubtful that appreciable plastic flow could be induced in quartz even at high temperatures, unless sintering temperatures (over 1000°C) were used. The hardness of quartz decreases with increasing temperature to about 700 Kg/mm^2 at 570°C (Westbrook, 1958). but the $\alpha - \beta$ inversion then occurs and the hardness increases to 2500 Kg/mm^2 (for as-yet unexplained reasons). At 700°C , the hardness is around 1000 Kg/mm^2 , which indicates that appreciably higher temperatures would be required to produce a hardness sufficiently low that the quartz would behave in a ductile manner.

D. The Frictional Behavior of Minerals

The available literature on the coefficient of friction for minerals is very small. The most comprehensive work to date is that by Horn (1961, Horn and Deere, 1962). Horn summarizes the

previous work, mostly on quartz, by Terzaghi (1925), Tschebotarioff and Welch (1948), and Penman (1953) among others.

All of these investigators, including Horn, found that the friction of quartz submerged in water was higher than in the dry condition by as much as a factor of 4 (0.11 dry vs. 0.42 wet). This anti-lubricating effect of water was found by Horn to apply to all three dimensional framework minerals that he tested.

Sir W. Hardy (1936, p. 518ff) ran a comprehensive series of tests on the friction of glass in which he investigated the effect of various lubricants. Hardy found that water did not change the value of μ for a clean glass surface (here clean refers to a surface free of dust and organic contamination). On an ordinary glass surface, water acted as an antilubricant because it interfered with the lubricating action of the invisible adsorbed organic films.

The amount of contamination required to cause a large drop in μ is extremely small. Holland (1964, p. 302) found that merely rubbing a linen cloth over a glass surface was sufficient to drop the coefficient of friction from 0.8 to 0.07. Other investigators have found that if a slider were being pulled across one end of a large sample, a minute amount of organic acid placed on the opposite end would immediately reduce the friction to a low value. Holland (1964, p. 379) also reports that the value of μ for a thin film of paraffin or castor oil on glass was increased by a factor of 4 when the surfaces were flooded with water.

The most likely explanation for the apparent anti-lubricating effect of water on quartz is that it disrupts the adsorbed lubricating films. If a clean quartz surface were prepared in a high vacuum, it would be expected to have a high μ , say 1.0. By adsorbing various materials onto this initially clean surface, their lubricating or anti-lubricating effect could be accurately determined.

Another possible explanation for the anti-lubricating effect of

water on quartz is as follows: the water attacks the silica surface, producing a silica gel or silicic acid which acts as a cement at the points of contact where it can solidify due to the high pressures. This has been shown to occur in some glasses, where the water hydrates alkali ions in the glass, forming an alkali solution which can readily attack the silica network (Holland, 1964, p.371). The insolubility of quartz to water and the absence of alkali ions would seem to prevent this mechanism from being a large factor for the short time of laboratory experiments. It may be of importance in the geologic formation of some cemented sands, however.

Horn also found that as the surface roughness increased, the apparent anti-lubricating effect of water decreased. Again this can be explained by assuming a thin organic film on the surfaces. For highly polished and uniform surfaces, only one or two molecular layers are required for effective lubrication. As the surface roughness increases, the thin organic film loses its effectiveness and more solid contact occurs through the film (Bowden and Tabor, 1950, p.114).

All of the surfaces used in Horn's work were relatively smooth. A 240 grit surface, the roughest he used, corresponds to about a 10 microinch finish. If the surface becomes very rough and the asperities are large compared with the area over which junctions are formed, then the interlocking effect must be considered. The force, F , required to raise a weight, W , up a plane inclined at an angle θ is

$$\frac{F}{W} = \tan \theta \quad (5.16)$$

Therefore, the total coefficient of friction, μ_+ , for a very rough surface should be of the form

$$\mu_+ = \mu_o + K \tan \theta \quad (5.17)$$

where μ_o is the value for a smooth surface, θ represents an average asperity angle, and K is an interlocking factor. K is less than one, because perfect interlocking will not occur. In fact, for even very

rough surfaces, the top surface may have very little vertical movement, and K may be close to zero.

Another major conclusion of Horn's work is that the friction of layer silicates (mica, talc, phlogopite, etc.) is lower in water than in air, the opposite behavior of that found for quartz. A reasonable explanation for this can be given by considering the water adsorption in the two cases. Horn noted that visible scratching occurred when these minerals were tested in air. This agrees with the heavy wear noted by Bailey and Courtney-Pratt (1955) when mica was tested in air, even though it had an adsorbed film on it. A layer of calcium stearate was found by Bailey and Courtney-Pratt to eliminate wear and greatly reduce the friction. In Horn's experiments, the submerged layer silicates probably adsorbed another layer (or more) of water, thereby reducing the amount of solid to solid contact, leading to less wear and reduced friction.

Friction as a Function of Interfacial Strength

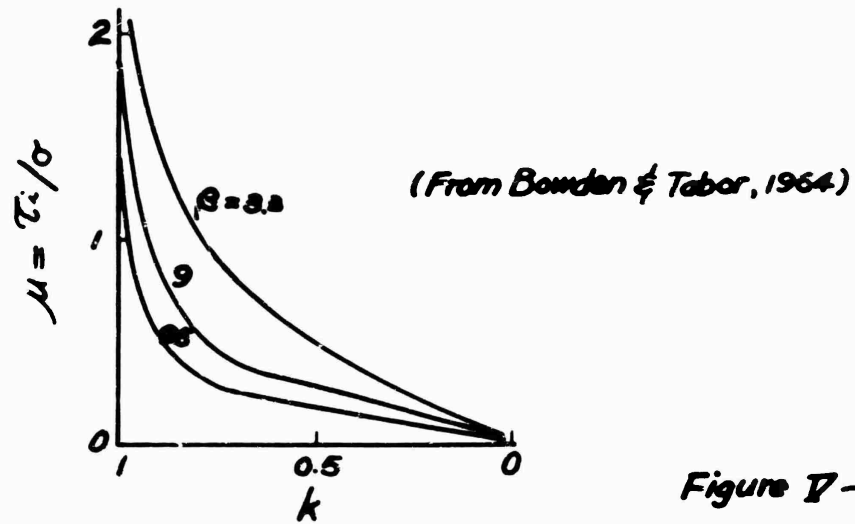


Figure IV-1

Area Increase vs. $\frac{F}{W}$

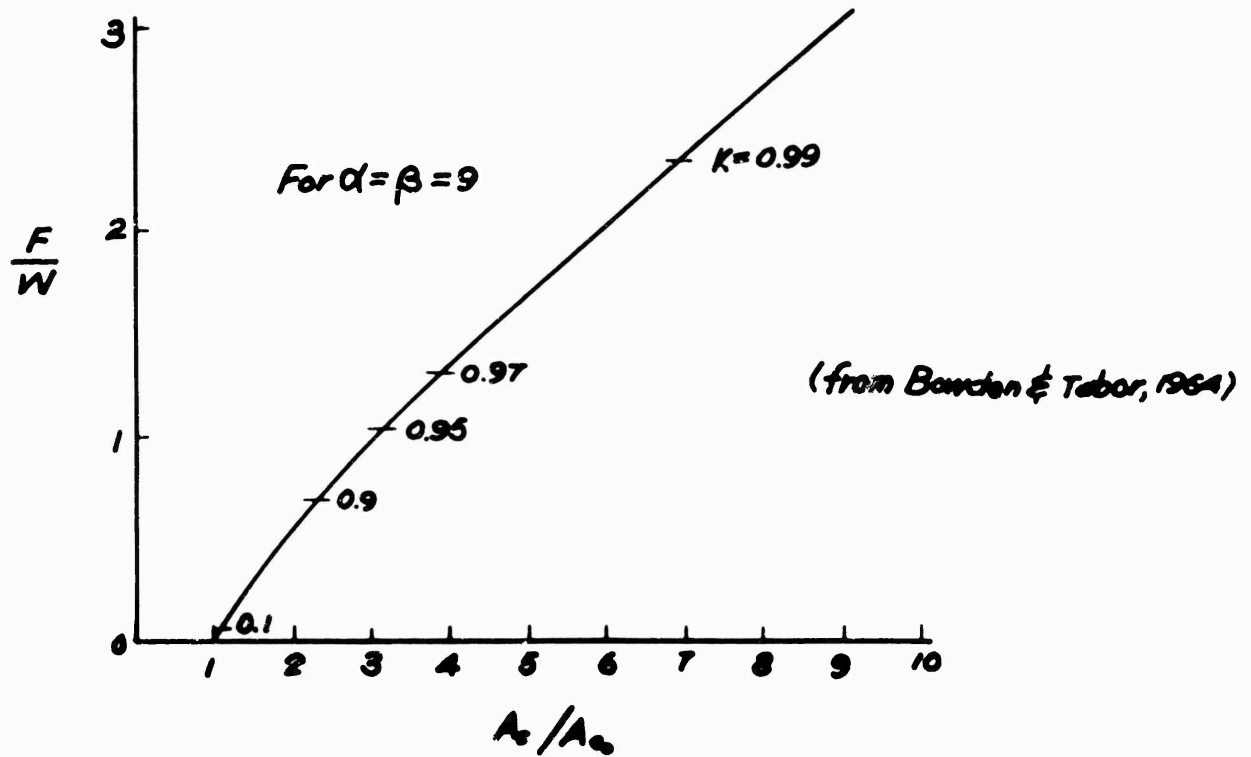


Figure IV-2

Variation of Friction with Particle Size

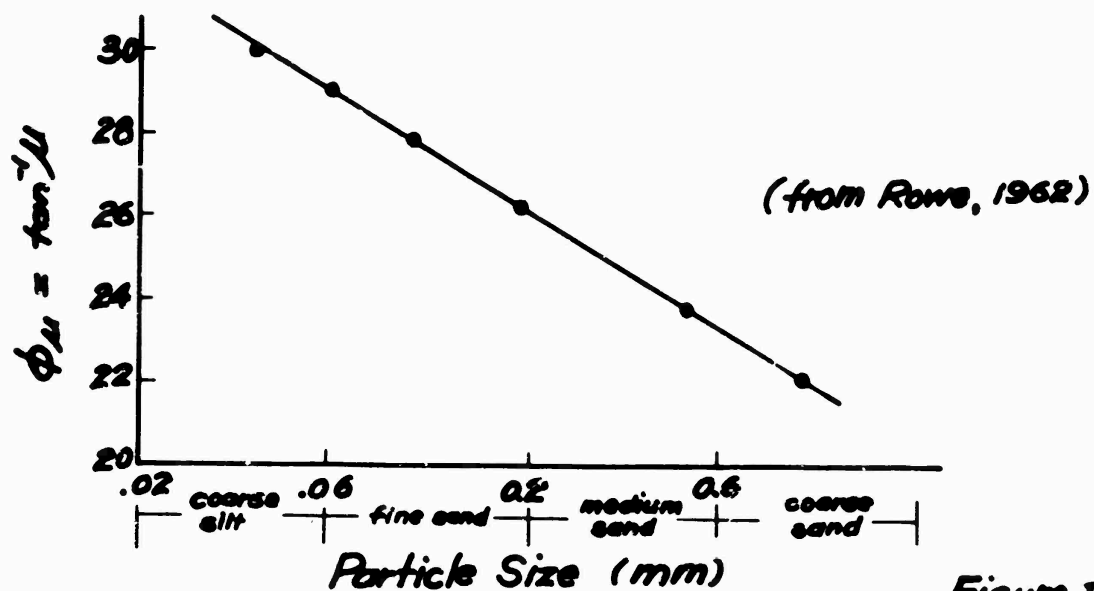


Figure V-3

Friction as a Function of Load per Particle

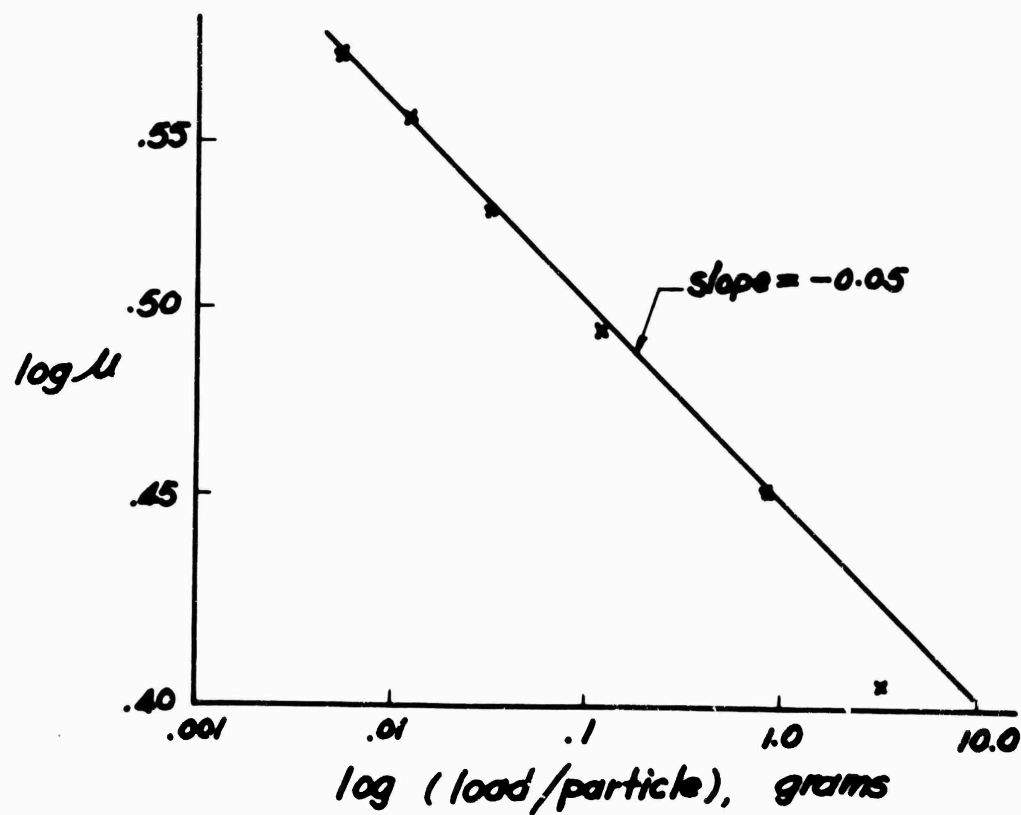


Figure V-4

Mohr Envelope for Quartz

data from Bridgman (1951)

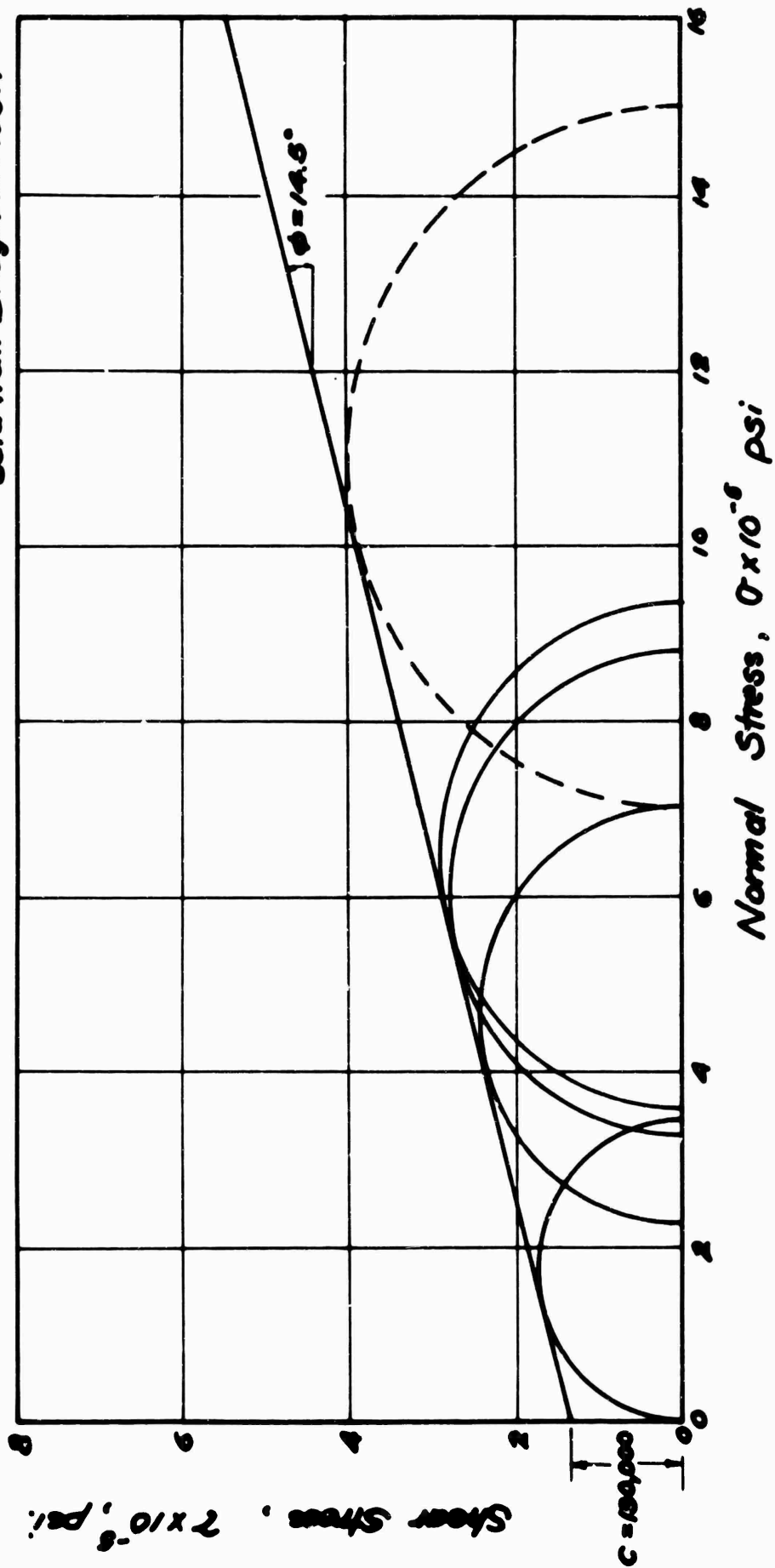


Figure D-5

Coefficient of Friction vs. Load for Mica

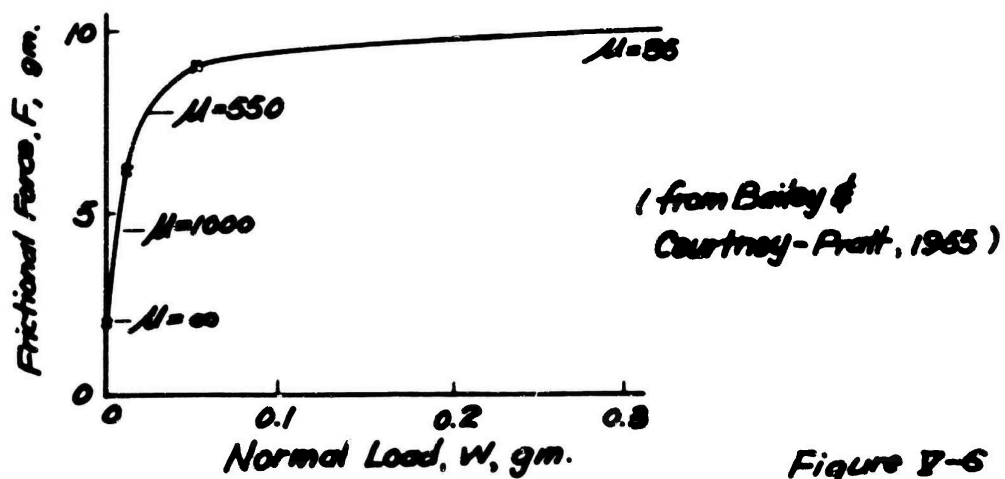


Figure 7-6

Area of Contact vs. Friction Force for Mica

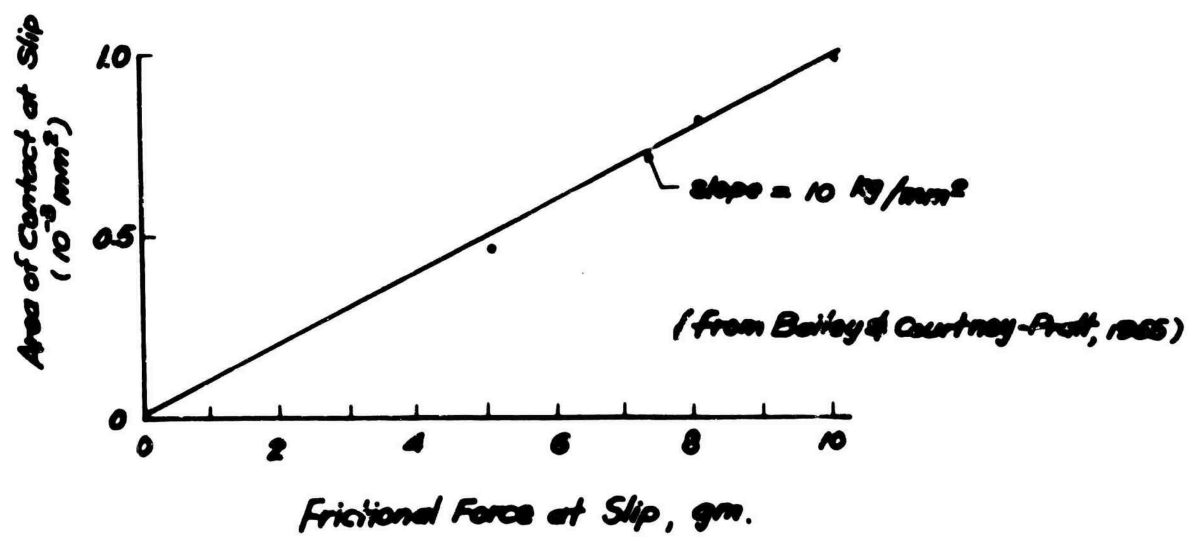


Figure 7-7

VI. PREVIOUS HIGH VACUUM RESEARCH ON SOILS

Since 1960 a large amount of work has been done on the high vacuum behavior of soils. Most of this work has been directed towards ascertaining the probable nature of the surface of the moon, where a vacuum of about 10^{-10} torr is thought to exist (Baldwin, 1963, Chapter 18, discusses the lunar atmosphere). Mitchell (1964) has summarized the previous and current research in this area. He notes about 30 current research projects on the nature of the lunar surface layer.

From a fundamental point of view, most of the published results of this research suffers from one or more of the following defects:

- 1) The tests did not measure parameters which permit quantitative interpretation of changes in soil properties. All of the early work, which consisted mainly of static and dynamic penetration tests, falls into this category. The emphasis now appears to have shifted to tests more likely to provide interpretable data, such as the direct shear test.
- 2) Vacuum levels were not high enough. This is a common problem because the large surface area of the soil samples used makes outgassing difficult and time consuming. The necessity of using high vacuum levels to obtain and maintain clean surfaces has been shown in this report.
- 3) Temperature variations were not considered. In addition to high vacuum, high bake-out temperatures generally must be used to desorb the surfaces. And unless the high temperature is maintained during testing, or the system is purged with a non-adsorbing gas, read-sorption will occur for most vacuum levels before the test is completed.

- 4) The system was poorly defined. Incomplete knowledge of the system cannot result in unequivocal interpretation of the data. To completely define the system requires knowledge of the surface being studied, its shape, roughness, and cleanliness. The residual gases present must be known, preferably by use of a mass spectrometer. The temperature and pressure in the soil must be measured if it may differ considerably from that in the chamber itself.

Two test programs have been reported which measured changes in the shear strength of soils under high vacuum. Both of these programs used direct shear tests.

Shear Strength of Soil Under High Vacuum

Sjaastad (1964) ran direct shear tests on glass spheres and nickel shot at 10^{-6} torr and up to 200°C . For glass, the Mohr-Coulomb friction angle ϕ_f increased from an atmospheric value of 32° to 43° under vacuum and elevated temperature. The coefficient of friction, μ , measured on plates of the same glass, increased from 0.12 ($\phi_{\mu} = 7^{\circ}$) to 0.49 ($\phi_{\mu} = 26^{\circ}$). These changes correspond to those measured by Horn (1961) on quartz in the air-dry and submerged condition. The effect of the vacuum and the temperature was to remove some of the adsorbed contamination which leads to the low friction measured in air.

The coefficient of friction was also measured for polished quartz surfaces. The quartz was cleaned by washing in benzene and acetone and was stored in a 70°C oven until used. The value of μ measured in air was 0.33, much higher than that reported by Horn (1961) and other investigators, indicating a higher degree of surface cleanliness than is normally obtained. When exposed to 10^{-5} torr vacuum and 200°C , the friction increased to 0.60. If the surfaces were allowed to cool in the vacuum, the friction remained at this

level, again indicating that the vacuum heating treatment had removed much of the remaining atmospheric contamination.

The cleaning effect of this vacuum treatment was also shown in the tests on nickel shot. The friction angle for direct shear increased from 45° to 55° in vacuum. Sjaastad anticipated a larger strength increase, particularly at the elevated temperature, and attributed the moderate values actually measured to incomplete cleaning of the surfaces.

Vey and Nelson (1963) have reported results of a large number of shear tests on powdered quartz and basalt at vacuum levels down to 8×10^{-10} torr and temperatures to 125°C . The soils used were fine grained, having 25% to 85% less than 10 microns, which caused difficult problems in outgassing the samples. Tests were run using a large sample with ionization gauges mounted at various levels to measure the pressure gradients in the soil (Courtney, Jamison, and Nelson, 1964). It was found that the pressure in the soil can be as much as two orders of magnitude higher than measured in the chamber.

Vey and Nelson generally found that the shear strength increased at high vacuum levels. The increases are moderate, involving changes in friction angle of only a few degrees. They have attempted to separate the strength increase into friction and cohesion components, but scatter of the data makes interpretation difficult.

In an interesting set of experiments, Vey and Nelson (1964), deposited silica flour onto various surfaces at 10^{-9} torr in order to study adhesion properties. No measurable adhesion occurred to glass or stainless steel, but small clusters of soil were found to cling to both teflon and aluminum plates. The soil on the aluminum could only be removed by scraping with a knife.

These results recall the conclusions of Bowden and Tabor (1964 p. 174) on the adhesion of diamond. Adhesion only occurs if one of the surfaces is able to flow plastically. No adhesion is

measured for diamond on diamond, but for diamond on platinum, values of μ as high as 3 are observed in a vacuum even at room temperature. Thus the quartz adherence to teflon and aluminum, both of which flow readily, may have been due to this mechanism. Presumably the stresses were not high enough to cause appreciable flow in the stainless steel or glass, and no large-scale junction growth occurred.

Stein and Johnson (1964) sifted fine crushed olivine and obsidian powders (80% $< 3\mu$) onto substrates of the same materials in high vacuum. At pressures around 10^{-10} torr and 100°C , adhesion was observed. By impacting the substrate it was found that an acceleration of about 12 g was necessary to dislodge the adhered grains. An exact stress analysis for this situation is not possible but cohesion clearly occurred in these tests.

By making what they considered reasonable assumptions, Stein and Johnson calculated a shear strength of 18,000 psi at the points of contact. However, the actual magnitude of the shear force was only about 3.2×10^{-2} dynes, which, based on the total area gave a cohesion of only 10^{-3} psi. This illustrates the necessity of having a large contact area, in addition to large cohesive forces, for a material to exhibit appreciable macroscopic cohesion.

Using similar materials, Halajian (1964) was able to induce adhesion between a rock powder and the wheels of a tumbling device which was used to thoroughly outgas the soil. Cohesion between particles also was observed. The source of the measured cohesion is not certain. It is convenient to use the plastic flow model developed for metals and attribute the cohesion to cold-welding. However, the arguments presented in this paper would seem to mitigate against cold-welding for brittle materials.

Gregg (1961, p. 252) states that research on dusts and dust explosions shows that small particles can easily become charged by

mixing, grinding, or sieving of powders. He cites the case of a powder falling through a chute at the rate of 1 lb./sec. where the charge generated is calculated as 10^{-7} coulombs/sec. If there is a high resistance to ground, say 10^{11} ohms, a voltage of 10,000 volts may quickly accumulate. It seems possible that electrostatic charges could have been present on the soil particles tested by Stein and Johnson and by Halajian as a result of the mechanical work done on the particles (in the grinding, sieving, and tumbling processes). Because of the small size of the particles, an accumulated electrostatic charge could have a large effect on their behavior.

Martin (1963) measured changes in the water vapor adsorption behavior of kaolinite after vacuum storage (10^{-5} torr) at 70°C for extended times (up to 6 months). Changes in the adsorption isotherm were related to changes in surface energy and total surface area by use of the BET equation. A reduction in both surface energy and surface area occurred for samples stored in high vacuum for more than 9 days, indicating particle coalescence. The permanence of the area reduction was verified by soaking samples in liquid water and by extracting with acidified Li Cl solution. Re-examination of the adsorption isotherm after treatment gave the same reduced surface area as before. The maximum area reduction measured was 14%. The shape of the kaolinite particles (small flat plates) probably contributed greatly to the coalescence. As was shown in Chapter V, extensive cold-welding requires a large contact area.

Clearly, more work is necessary to determine whether or not clean soil surfaces will cold-weld and the conditions required for this to occur. Accurate measurements of the actual magnitude of tensile force required to separate "stuck" particles would help answer many unresolved questions.

VII. CONCLUSIONS

1. To prepare and maintain clean surfaces, ultra-high vacuums of 10^{-10} torr and temperatures between 200°C and 500°C must generally be used.
2. The degree of cleanliness of a vacuum is as important as the pressure level. Pressures of 10^{-10} torr can be useless for maintaining clean surfaces if the gas composition includes appreciable organic vapor.
3. It is necessary to know or to be able to estimate accurately the composition of the residual gas in a high vacuum system. Exact analysis requires a mass spectrometer. Various techniques, such as wettability of a surface and flushing with a rare gas may be used to estimate the cleanliness of the system.
4. The surfaces of most solids vary so far from ideality that interpretation of experimental data is very difficult. Cleaving of a solid in a high vacuum will provide the closest possible approach to an ideal surface.
5. The low surface energy normally measured for quartz probably results from adsorbed contamination. Removing these contaminants may produce a high energy surface. On the other hand, the conditions required for removal may drastically alter the surface structure, resulting in a very low energy surface.
6. A desorption equation relating the pressure and temperature to the adsorption energy has been derived. This equation and the accompanying curves can be used to help determine the conditions required to clean a given solid surface.
7. The question of whether quartz asperities deform plastically or elastically is difficult to determine. Undoubtedly, some plastic flow can occur for at least a few asperities. However, it seems likely that the stress usually carried by an asperity on an "average" surface, whether this be a quartz block or a granular particle, is not high enough for plastic flow to occur.

8. **Regardless of the cleanliness of the surfaces or the magnitude of the surface forces, extensive cold-welding can only occur if there is a large contact area. A mechanism whereby quartz particles could develop a large contact area below 1000°C is difficult to envision.**
9. **Cases of observed cohesion between granular soil particles do not provide clear-cut evidence of cold-welding. Measurements of tensile strength between "stuck" particles which have no accumulated electrostatic charge are necessary to resolve this question.**

VIII. LITERATURE CITED

1. Adamson, A.A. (1960). Physical Chemistry of Surfaces, Interscience Publishers, New York.
2. Archard, J.F. (1957). "Elastic Deformation and the Laws of Friction", Proceedings of the Royal Society, A243, pp. 190-205.
3. Bailey, A.I. and Courtney-Pratt, J.S. (1955). "The Area of Real Contact and the Shear Strength of Monomolecular Layers of a Boundary Lubricant", Proc. Roy. Soc., A227, pp. 500-515.
4. Baldwin, Ralph R. (1963). The Measure of the Moon, Univ. of Chicago Press, Chicago Illinois.
5. Bastow, S.H. and Bowden, F.P. (1932). "On the Contact of Smooth Surfaces", Proc. Roy. Soc., A134, pp. 404-413.
6. _____ (1935). "Physical Properties of Surfaces II - Viscous Flow of Liquid Films. The Range of Action of Surface Forces", Proc. Roy. Soc., A151, pp. 220-233.
7. Becker, J.A. (1958). "Study of Surfaces by Using New Tools", in Solid State Physics, V.7, pp. 379-424, Academic Press, New York.
8. Belofsky, H. (1962). "Mechanics of the Evacuation-Purging Cycle for Sealed Chambers", Review of Scientific Instruments, 33, pp. 1121-1122.
9. Bishop, A. W. (1954). Correspondence on "Shear Characteristics of a Saturated Silt, Measured in Triaxial Compression." Geotechnique, 4, pp. 43-45.
10. Bowden, F. P. and Tabor, D. (1950). The Friction and Lubrication of Solids, Part I, Oxford Univ. Press, London.
11. _____ (1957). "Mechanism of Adhesion between Solids", Proc. 2nd Inter. Conf. on Surface Activity, Academic Press, N.Y.
12. _____ (1964). The Friction and Lubrication of Solids, Part II, Oxford Univ. Press, London.

13. Bowden, F.P. and Throssell, W.R. (1951). "Adsorption of Water Vapour on Solid Surfaces", Proc. Roy. Soc., A209, pp. 297-308.
14. _____ and Young, J.E. (1951). "Friction of Clean Metals and the Influence of Adsorbed Films", Proc. Roy. Soc., A208, pp. 311-325.
15. Brace, W.F. (1960). "Behavior of Rock Salt, Limestone, and Anhydrite during Indentation", J. of Geophysical Research, V. 65, No.6, pp. 1773-1788.
16. _____ and Walsh, J.B. (1962). "Some Direct Measurements of the Surface Energy of Quartz and Orthoclase", American Mineralogist, 47, pp. 1111-1122.
17. _____ (1963). "Behavior of Quartz during Indentation", The Journal of Geology, V.71, No.5, pp. 581-595.
18. Bridgman, P.W. (1952). Studies in Large Plastic Flow and Fracture, McGraw-Hill Book Co., Inc., N.Y.
19. Brunauer, S. (1945). The Adsorption of Gases and Vapors, Princeton Univ. Press, Princeton, N.J.
20. Bryant, P.J. (1962). "Cohesion of Clean Surfaces and the Effect of Adsorbed Gases", Proc. of the 9th Nat. Vacuum Symposium, pp. 311-313, Macmillan Co., N.Y.
21. Caquot, A. (1934). Equilibre des Massifs a Frottement Interne. Stabilite des Terres Pulvérulents eu Cohérentes. Gauthier-Villars, Paris.
22. Courtney, W.J., Jamison, W.E. and Nelson, J.D. (1964). "Pore Pressure Profiles in Simulated Lunar Soils", paper presented at the 11th Nat. Vacuum Symposium, Chicago, Ill., October 1964.
23. Davis, W.D. (1962). "Sputter - Ion Pumping and Partial Pressure Measurements Below 10^{-10} Torr", Proc. of the 9th Nat. Vacuum Symposium, pp. 363-370, Macmillan Co., N.Y.
24. Dempster, P.B. and Ritchie, P.D. (1953). "Physicochemical Studies of Dusts V. Examination of Finely Ground Quartz by DTA and Other Physical Methods", J. of Applied Chemistry, 3, pp. 182-192.

25. Derjaguin, B.V. and Zorin Z. M. (1957). "Optical Study of the Adsorption and Surface Condensation of Vapors in the Vicinity of Saturation on a Smooth Surface", Proc. 2nd Inter. Conf. on Surface Activity, Academic Press, N.Y.
26. Ehrlich, G. (1959). "Molecular Processes at the Gas-Solid Interface", in The Structure and Properties of Thin Films, edited by Neugebauer, C.A., Newkirk, J.B., and Vermilyea, D.A., John Wiley and Sons, N.Y.
27. Gatos, H.C. (1962). "Crystalline Structure and Surface Reactivity", Science, 137, No. 3527, pp. 311-322.
28. Gregg, S.J. (1961). The Surface Chemistry of Solids, 2nd Edition, Reinhold, N.Y.
29. Griffith, A.A. (1920). "The Phenomenon of Rupture and Flow in Solids", Phil. Trans. Roy. Soc. London, A221, pp. 163-198.
30. Halajian, J.D. (1964). "The Case for a Cohesive Lunar Surface Model", Grumman Aircraft Eng. Corp., Report No. ADR-04-04-64.2.
31. Hardy, Sir. W.B. (1936). Collected Works, Cambridge Univ. Press.
32. Holland, L. (1964). The Properties of Glass Surfaces, John Wiley and Sons, Inc., N.Y.
33. Horn, H.M. (1961). An Investigation of the Frictional Characteristics of Minerals, ScD. Thesis, Univ. of Ill. Urbana, Ill.
34. _____ and Deere, D.U. (1962). "Frictional Characteristics of Minerals", Geotechnique, 12, pp. 319-335.
35. Iler, R.K. (1955). The Colloid Chemistry of Silica and Silicates, Cornell Univ. Press, Ithaca, N.Y.
36. King, R.F. and Tabor, D. (1954). "The Strength Properties and Frictional Behavior of Brittle Solids", Proc. Roy. Soc., A223, pp. 225-238.
37. Martin, R.T. (1960). "Adsorbed Water on Clay: A Review", in Clays and Clay Minerals, V.9. pp. 28-67, Pergamon Press, N.Y., 1962.

38. Martin, R.T. (1963). "Water Vapor Adsorption Behavior of Kaolinite after High Vacuum Storage", in The Lunar Surface Layer, edited by J.W. Salisbury and P.E. Glaser, Academic Press, N.Y., 1964.
39. Michaels, A.S. (1962). "Fundamentals of Surface Chemistry and Surface Physics", Symposium on Properties of Surfaces, Special ASTM Tech. Publ. No. 340.
40. Mitchell, James K. (1964). "Current Lunar Soil Research", Proc. of the A.S.C.E., Soil Mechanics and Foundations Division, V. 90, No. SM3, pp. 53-83.
41. Nadai, A. (1950). Theory of Flow and Fracture of Solids, McGraw-Hill Book Co., Inc., N.Y.
42. Newland, P.L. and Allely, B.H. (1957). "Volume Changes in Drained Triaxial Tests on Granular Materials", Geotechnique, 7, pp. 17-34.
43. Pauling, L. (1960). The Nature of the Chemical Bond, 3rd Edition, Cornell Univ. Press, Ithaca, N.Y.
44. Penman, A.D.M. (1953). "Shear Characteristics of a Saturated Silt, Measured in Triaxial Compression", Geotechnique, 3, pp. 312-328.
45. Rabinowicz, E. (1961). "Influence of Surface Energy on Friction and Wear Phenomena", J. of Applied Physics, V.32, No.8, pp. 1440-1444.
46. Roberts, R.W. and Vanderslice, T.A. (1963). Ultra-High Vacuum and Its Applications, Prentice-Hall Inc., Englewood Cliffs, N.J.
47. Rowe, P.W. (1962). "The Stress-Dilatancy Relation for Static Equilibrium of an Assembly of Particles in Contact", Proc. Roy. Soc., A269, pp. 500-527.
48. Schofield, R.K. (1935). "The pF of the Water in Soil", Trans. Third Int. Cong. of Soil Science, V.2, pp. 37-48.
49. Sjaastad, G.D. (1964). "An Experimental Study in Lunar Soil Mechanics", in The Lunar Surface Layer, edited by J.W. Salisbury and P.E. Glaser, pp. 23-65, Academic Press, N.Y.
50. Skempton, A.W. (1960). "Effective Stress in Soils, Concrete, and Rocks", in Pore Pressure and Suction in Soils, Butterworths, London.

51. Sonntag, A. (1961). "Boundary Friction and Lubrication by Solids", presented at the Annual Meeting of the A.S.L.E., Philadelphia, Pa., April 1961.
52. Stein, B.A. and Johnson, P.C. (1964). "Investigation of Soil Adhesion Under High Vacuum", in The Lunar Surface Layer, edited by J.W. Salisbury and P.E. Glaser, pp. 93-109, Academic Press, N.Y.
53. Tabor, D. (1956). "The Physical Meaning of Indentation and Scratch Hardness", British Journal of Applied Physics, 7, pp. 159-166.
54. Terzaghi, K. (1925). Erdbaumechanik, Franz Deuticke, Vienna.
55. Thompson, J.B., Washburn, E.R. and Guildner, L.A. (1952). "Adsorption of Carbon Dioxide by Glass", J. Phys. Chem. 56, pp. 979-984.
56. Timoshenko, S. and Goodier, J.N. (1951). Theory of Elasticity, McGraw-Hill Book Co., Inc., N.Y.
57. Tschebotarioff, G.P. and Welch, J.D. (1948). "Lateral Earth Pressures and Friction Between Soil Minerals", Proc. 2nd Int. Conf. Soil Mech. and Fdn. Eng., V.7, pp. 135-138.
58. van Olphen, H. (1963). "Compaction of Clay Sediments in the Range of Molecular Particle Distances", in Clays and Clay Minerals, V.13, pp. 178-187. Pergamon Press, N.Y. 1963.
59. Verwey, E.J.W. and Overbeek, J. ThG. (1948). Theory of the Stability of Lyophobic Colloids, Elsevier Publishing Co., Amsterdam.
60. Vey, E. and Nelson, J.D. (1963). "Studies of Lunar Soil Mechanics", Final Report for NASA, Contract No. NASr-65(02).
61. _____ (1964). "Studies of Lunar Soil Mechanics", Fifth Quarterly Progress Report, IITRI Project No. M272, Phase II.
62. Westbrook, J.H. (1958). "Temperature Dependence of Strength and Brittleness of Some Quartz Structures", J. Amer. Ceramic Society, 41, pp. 433-440.

- 6 . Young, J. R. and Whetten, N. (1963). "Purity of Helium Permeating Through Quartz Into a Vacuum System", Rev. Sci. Instr., 32, pp. 453-454.

APPENDIX I

PURGING ACTIVE GASES FROM HIGH VACUUM SYSTEMS

Consider a chamber of volume V , filled with molecules of type B at an initial pressure p_{Bi} . Molecules of type A flow into the chamber and mix perfectly with B. Assuming ideal gas behavior, constant temperature, and constant total pressure, the flow rates of A and B leaving the chamber are proportional to their respective concentrations within the chamber:

$$(dA_2/dt) / (dB_2/dt) = \frac{A}{B} \quad (1)$$

$A + B$ = total number of molecules/cm³ in chamber

A_2, B_2 = number of molecules/cm³ in stream leaving chamber.

The net flux of A molecules into V is given by:

$$dA/dt = q_A - (dA_2/dt) \quad (2)$$

where

q_A = flow rate (molecules/cm²/sec) of A into chamber

The net flux of B molecules is given by:

$$dB/dt = q_B - (dB_2/dt) \quad (3)$$

To get a solvable differential equation, we assume that no B molecules are in the incoming gas stream, i.e., $q_B = 0$. The condition $q_B \neq 0$ can be handled in a manner described later.

Since the total pressure is constant, Avogadro's Law gives

$$A + B = N \quad (4)$$

where N is the total number of molecules/cm³ in the chamber at any time t .

Differentiating (4) gives

$$\frac{dA}{dt} = - \frac{dB}{dt} \quad (5)$$

Substituting (5) into (2) leads to

$$q_A - \frac{dA_2}{dt} = - \frac{dB}{dt} \quad (6)$$

Substituting into (6) the value of $\frac{dA_2}{dt}$ in equation (1):

$$q_A - \frac{A}{B} \left(\frac{dB_2}{dt} \right) = - \frac{dB}{dt} \quad (7)$$

For $\left(\frac{dB_2}{dt} \right)$ in equation (7), substitute from equation (3):

$$q_A + \frac{A}{B} \left(\frac{dB}{dt} \right) = - \frac{dB}{dt} \quad (8)$$

Solving this simple first-order equation gives a formula for the number of molecules of type B remaining in the chamber after an elapsed time t during which there has been a constant flow q_A , of type A molecules:

$$B = N \exp (- q_A t / N) \quad (9)$$

$\frac{q_A t}{N}$ is equivalent to the number of complete changes of atmosphere in time t .

To illustrate the use of equation (9), the example used in the text, page 20, will be calculated.

Example Calculation

A vacuum chamber is evacuated to 1×10^{-8} torr at 300°K . If the remaining gas is considered to be oxygen, the number of molecules present, N , will be given by

$$N = 9.67 \times 10^{18} \frac{p}{T} = 3.22 \times 10^8 \text{ molecules/cm}^3$$

If Helium gas containing 2 ppm of oxygen as an impurity is now flushed through at a constant pressure of 1×10^{-8} torr until 10 volumes of helium have been bled in, $\frac{qt}{N} = 10$, and

$$\frac{B}{N} = \exp (- q_{\text{He}} t / N) = e^{-10} = 4.5 \times 10^{-5}$$

Therefore

$$B = (4.5 \times 10^{-5})(3.22 \times 10^8) = 1.45 \times 10^4 \text{ molecules/cm}^3$$

That is, 1.45×10^4 molecules/cm³ of the original oxygen will still be in the chamber. The amount of oxygen which was added with the helium is given by

$$\begin{aligned} N_{\text{add}} &= \text{ppm}_{\text{O}_2} \times N \times \text{no. of purge cycles} \\ &= (2 \times 10^{-6})(3.22 \times 10^8)(10) \\ &= 6.44 \times 10^3 \end{aligned}$$

The final concentration of oxygen is thus

$$N_{\text{O}_2} = (1.45 + .64) \times 10^4 = 2.09 \times 10^4 \text{ molecules/cm}^3$$

If the chamber is now pumped down to a total pressure of 1×10^{-10} torr, the oxygen concentration will be

$$N_2 = N_1 \frac{p_2}{p_1} = 2.09 \times 10^4 \frac{10^{-10}}{10^{-8}} = 2.09 \times 10^2 \text{ molecules/cm}^3$$

This corresponds to a partial pressure of oxygen of

$$p_{\text{O}_2} = \frac{N T}{9.67 \times 10^{13}} = 6.5 \times 10^{-15} \text{ torr}$$

which is an extremely low pressure.

APPENDIX II

KINETICS OF SURFACE DESORPTION

Adsorption is a dynamic process, with gas molecules constantly arriving at and leaving the surface. Equilibrium is always achieved by equating the number of arriving molecules per unit area to the number of departing molecules per unit area. If the average time of residence, τ , is very large, the time scale will be greatly expanded and the dynamical nature becomes more a mathematical convenience than an observable phenomenon.

To prevent appreciable adsorption on a surface, the average residence time must be very small compared to the time required for a new molecule to arrive at a given surface site. If the concentration of molecules on the surface is taken as Γ molecules/cm², then

$$\Gamma = Z\tau \quad (1)$$

where Z is the rate of arrival of molecules to the surface, molecules/cm²/sec. and τ is the average residence time in seconds.

Z is given by kinetic theory (Brunauer, p.61):

$$Z = \frac{pN}{(2\pi MRT)^{1/2}} \quad (2)$$

where

p = Pressure of the gas

N = Avogadro's number

M = Molecular weight of the gas

R = Universal Gas constant

T = Absolute Temperature, °K

for water vapor,

$$Z = 8.3 \times 10^{21} \frac{p}{\sqrt{T}} \quad (3)$$

where p is measured in mm. of Hg.

Γ may also be expressed in terms of the concentration of molecules per surface site. Since monomolecular coverage for

water corresponds to about 1.2×10^{15} molecules/cm², this leads to

$$Z^1 = \frac{Z}{1.2 \times 10^{15}} = 6.9 \times 10^6 \frac{p}{\sqrt{T}} \quad (4)$$

and

$$\Gamma^1 = Z^1 \tau \quad \text{Molecules / Surface site / sec.} \quad (5)$$

τ is given by an Arrhenius type equation:

$$\tau = \tau_0 \exp (Q/RT) \quad (6)$$

where $\tau_0 = 10^{-13}$ sec. = time for a specular reflection

Q = adsorption energy, Kcal/mole

For no adsorption, we would naturally require $\Gamma^1 = 0$.

However, this is an impossible situation which requires either zero pressure or infinite temperature. As a practical matter, we can take $\Gamma^1 = 1$, which corresponds to just maintaining a monolayer on the surface. If the temperature is raised slightly, Γ^1 will be less than 1, requiring infinite time for formation of a monolayer. If in addition Z^1 is at least an order of magnitude less than τ , the assumptions will lead to reasonable results, for most of the surface sites will be vacant most of the time.

Combining equations (4), (5), and (6) leads to an equation relating Q , p , and T as follows:

$$\begin{aligned} \Gamma^1 &= Z^1 \tau \\ 1 &= (6.9 \times 10^6 \frac{p}{\sqrt{T}}) [10^{-13} \exp (Q/RT)] \end{aligned}$$

which gives, with sufficient accuracy for this analysis,

$$\frac{p}{\sqrt{T}} \exp (Q/RT) = 10^6 \quad (7)$$

Taking the \log_e of both sides of equation (7)

$$2.3 \times 6 = \ln p - \frac{1}{2} \ln T + Q/RT$$

or

$$Q = T \ln T + 4.6 T (6 - \log_{10} p) \quad (8)$$

Since $T \ln T$ is generally less than 10% of Q , an approximate equation for temperatures between 200°K and 2000°K is

$$Q = 5.1 T (6 - \log_{10} p) \quad \text{cal/mole} \quad (9)$$

A plot of equation (8) is given in Fig. IV-3. Independent confirmation of the general validity of this derivation appears to be given by Becker (1958). He measured the adsorption of various gases on a small tungsten ribbon, and by use of a fast-responding ion gauge was able to calculate the number of molecules desorbed when the ribbon was quickly heated to a temperature T . Becker gives the adsorption energy, Q , in electron volts/molecule as

$$Q = \frac{T}{350} \quad \text{e.v.}$$

where T is the absolute temperature at which desorption occurred. Becker gives no indication of how this equation was derived. However, it can be shown to correspond to equation (9) derived earlier in this appendix. Since $1 \text{ e.v.} = 23 \text{ Kcal/mole}$, Becker's equation may be written as

$$Q = \frac{T}{15.2} \quad \text{Kcal/mole}$$

The pressures used in Becker's experiments were around 10^{-7} torr which, when put into equation (9) gives

$$10^3 Q = 5.1 T [6 - (-7)] = 67.5 T$$

$$Q = \frac{T}{14.8}$$

which agrees very well with Becker's value.